



Most of the material can be found in textbooks. I recommend these for further reading:

Aerodynamics of Road Vehicles by Wolf-Heinrich Hucho

Race Car Aerodynamics by Joseph Katz

Road Vehicle Aerodynamic Design by R. H. Barnard

All Images are © Aerolab, CUED unless otherwise stated.

Holger Babinsky, February 2016

1. Review of previous material

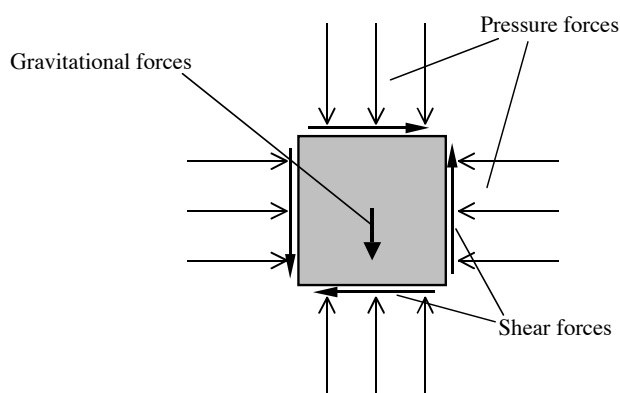
Everything contained in this section is effectively a repeat of material previously covered in Part I and 3A1. I am likely to cover this ground quickly but there is more detail here for background reading.

The relationship between forces and streamlines

Here we will consider the forces acting on individual fluid particles and from an understanding of these forces derive the streamline pattern in a flow. Vice versa, this will allow us to look at the streamline pattern in a flow and make an educated guess as to what the forces are like – which is very useful when we want to estimate the pressures and skin friction acting on the surface of a vehicle. This approach may not provide exact quantitative answers but it should give you the ability to get a feel for the order of magnitude of flow quantities and also an understanding of what causes certain flow patterns (and how to change them).

To begin with we need to consider what forces act on a fluid particle. Typical forces include:

- Gravity
- Pressure forces
- Shear forces

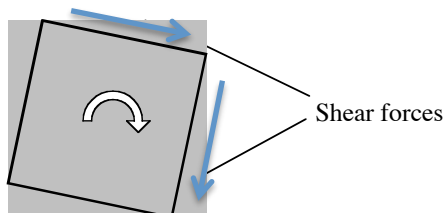


The sum total of all forces acting on a particle (keeping in mind that these are vector quantities) causes an acceleration of this particle according to Newton's second law:

$$F = m \times a$$

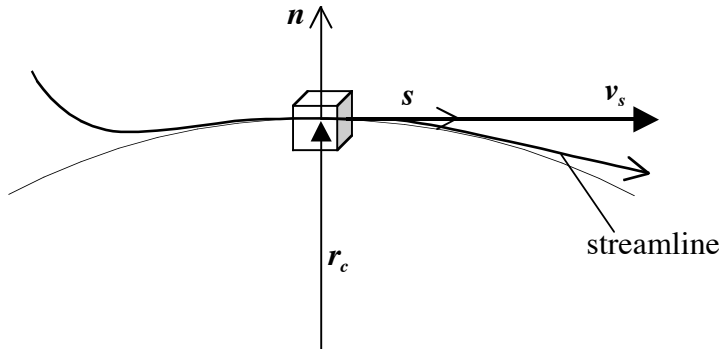
For example, in hydrostatics we assumed that there was no fluid motion (and hence no acceleration). In this case the pressure forces balance the gravitational forces which leads to $p=\rho gh$.

Note, that frictional forces do not act through the centre of mass of the fluid element and they are therefore able to impart 'twist', making it rotate. *Irrational* flows are therefore inviscid.



Acceleration of a fluid particle

In 3A1 we primarily consider fluid flow at velocities well below the speed of sound of the fluid and this means that we can treat the fluid as incompressible ($\rho=\text{constant}$). However, we do not restrict ourselves to steady flow. Imagine a fluid particle moving along a random streamline (which may change with time if the flow is unsteady):



We are considering the motion in intrinsic coordinates (s, n) where s is in the direction of the streamline and n is the direction normal to it. Because a streamline is defined as being tangential to the local velocity vector, the particle velocity V is equal to its component in streamline direction v_s and $v_n = 0$.

Assuming that the streamline has a local radius of curvature r_c (this does not mean the streamline must be circular), we can write the particle acceleration in s and n direction as follows:

$$\begin{aligned} s - \text{coordinate: } & \frac{\partial v_s}{\partial t} + v_s \frac{\partial v_s}{\partial s} \\ n - \text{coordinate: } & \frac{\partial v_n}{\partial t} - \frac{v_s^2}{r_c} \end{aligned}$$

In *steady* flow both $\partial v_s / \partial t$ and $\partial v_n / \partial t$ are zero and we obtain:

$$\begin{aligned} \text{Acceleration in streamwise direction: } & v_s \frac{\partial v_s}{\partial s} \equiv V \frac{\partial V}{\partial s} \\ \text{Acceleration normal to streamlines: } & \frac{v_s^2}{r_c} \equiv \frac{V^2}{r_c} \end{aligned}$$

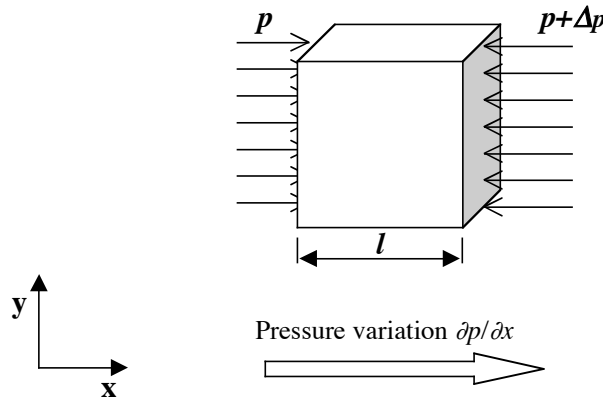
(where V is the local fluid velocity).

Inviscid flow

For now we will ignore viscous forces.

Pressure forces acting on a fluid particle

As a further simplification we will also neglect gravity. In this case the only forces acting on a fluid particle are caused by pressure and consequently the pressure forces must balance the inertial forces.



In 1A Thermofluids you have learned that a fluids particle exposed to a pressure gradient experiences a body force in the opposite direction of the gradient. Applied to the above, this gives:

$$\mathbf{F}_x = -Vol \frac{\partial p}{\partial x}$$

Similarly, by returning to our streamline coordinate system (s, n):

$$\mathbf{F}_s = -Vol \frac{\partial p}{\partial s}$$

$$\mathbf{F}_n = -Vol \frac{\partial p}{\partial n}$$

To apply Newton's 2nd law ($\vec{F} = m \times \vec{a}$) we need the mass of the particle:

$$m = \rho \times Vol$$

and combining this with the accelerations derived earlier allows us to write (for steady flow):

$$\text{s-coordinate: } -\frac{\partial p}{\partial s} Vol = V \frac{\partial V}{\partial s} \rho Vol$$

$$\text{n-coordinate: } -\frac{\partial p}{\partial n} Vol = -\frac{V^2}{r_c} \rho Vol$$

or, more simply:

$$\text{s-coordinate: } \frac{\partial p}{\partial s} + \rho V \frac{\partial V}{\partial s} = 0$$

$$\text{n-coordinate: } \frac{\partial p}{\partial n} - \rho \frac{V^2}{r_c} = 0$$

which is beginning to look familiar. The second part of this equation was already introduced in 1A Thermofluid mechanics to investigate the pressure gradient across curved streamlines:

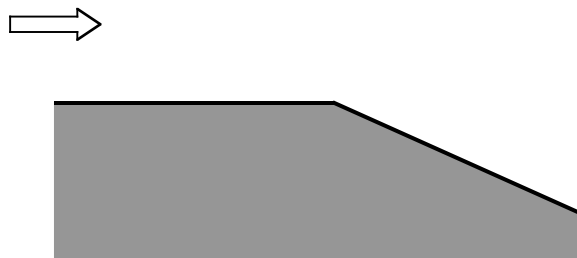
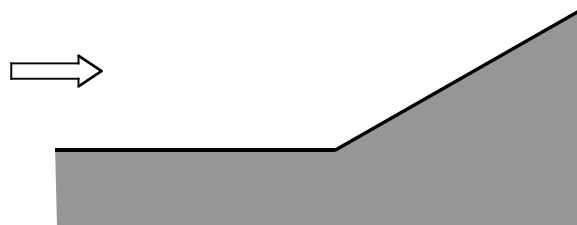
$$\frac{\partial p}{\partial n} = \rho \frac{V^2}{r}$$

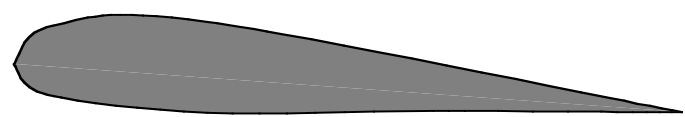
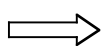
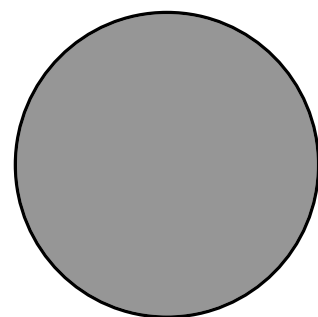
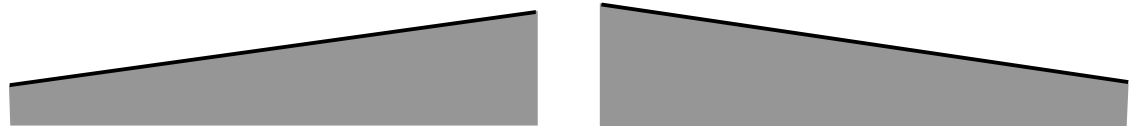
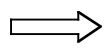
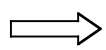
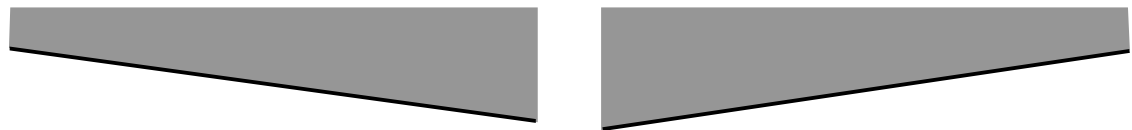
The first can be integrated along s to give:

$$p + \frac{1}{2} \rho V^2 = \text{const.}$$

which is the well known Bernoulli's equation along a streamline. Here we have ignored gravity but the derivation can almost as easily be performed with a gravitational force included (which leads to the equivalent term in Bernoulli's equation).

Now we have the tools to determine the pressure field in a flow from a knowledge of streamline shape. Along streamlines we can use Bernoulli's equation or the s -component of the Euler equation. Between neighbouring streamlines we can use the n -component of the Euler equations. By simply drawing some streamlines (which we can guess) it is possible to determine the pressure field.



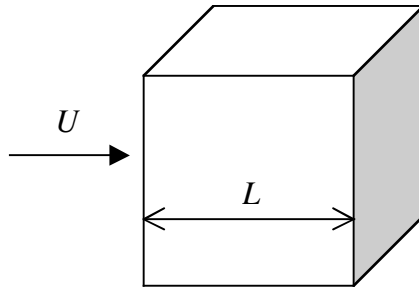


Viscous effects

From the previous sections you should now be able to guess the pressure field from a knowledge of streamline shapes or vice versa, as long as the flow is inviscid. Now we want to see to what extent the picture is changed if we include viscous forces. In this case:

$$\text{Change of momentum} = \text{pressure forces} + \text{viscous forces}$$

We have already seen that viscous forces depend on the velocity gradient and the coefficient of viscosity μ . The latter is very small for practical fluids such as air and water ($\approx 10^{-5}$ and 10^{-3} kg/ms respectively) and we might wonder whether viscous forces actually matter. To put this into perspective, let us find the approximate contribution of viscous forces to the inertial forces in a flow by determining their relative *orders of magnitude* (this is quite a rough estimate but bear with me for now). Consider a general flowfield which has a typical dimension, or length scale, L and a typical velocity U :



In this case, the order of magnitude of a typical area is

$$A = L^2$$

Consequently, a typical mass flow rate is:

$$\dot{m} \approx \rho L^2 U$$

First we estimate the order of magnitude of the inertial force using the steady flow momentum equation:

$$F_{inertia} = \dot{m} \Delta V = \rho L^2 U (U - 0) = \rho L^2 U^2$$

Next we estimate the order of magnitude of a typical viscous force:

$$F_{viscous} = A \tau = L^2 \mu \frac{\partial V}{\partial y} = L^2 \mu \frac{U}{L} = \mu U L$$

The ratio of the two forces becomes:

$$\frac{F_i}{F_v} = \frac{\rho L^2 U^2}{\mu U L} = \frac{\rho U L}{\mu} = Re_L$$

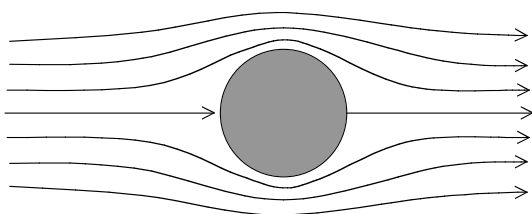
We see that the order of magnitude of the ratio between inertial forces and viscous forces in a flow is expressed by the Reynolds number.

In many practical flowfields the Reynolds number is of the order of $10^2 \dots 10^7$. Very large Reynolds numbers suggest that pressure forces are much larger than viscous forces. In other words, the fluid

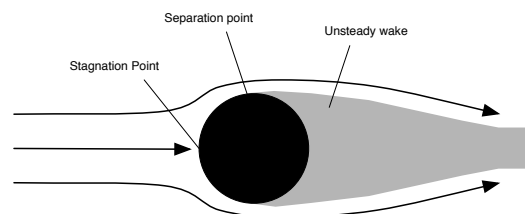
acceleration is primarily determined by the pressure field (and the pressure field primarily determines the fluid motion). This explains why the treatment of many flows as inviscid can give such good results.

Does the fact that most practical flow problems feature large Reynolds numbers mean that we can neglect viscous forces altogether? The French scientist Jean d'Alembert puzzled over this problem (allegedly). He had experienced the success of the theory of inviscid flow (in the form of potential flow which was discussed earlier in 3A1) in describing realistic flow patterns while failing to predict drag. In fact he even proved analytically that if a body is immersed into an irrotational, inviscid flow there is *no drag*. On the other hand, he was well aware that objects immersed into a flow do certainly experience drag forces. Even at high Reynolds numbers these are often quite substantial and well above the negligible level suggested by the order of magnitude analysis shown earlier. He could not solve this conundrum which is now referred to as “d'Alembert's paradox”. The problem he saw was that he could not explain how viscosity, whose effects ought to be negligible at high Reynolds numbers, could generate the sizeable drag forces seen in practice (because inviscid flow cannot generate drag).

However, we often see that viscous forces do make a big difference not only in generating a drag force but also in changing the overall flow pattern. A comparison of the inviscid and ‘real’ flow around a circular cylinder illustrates this very well.



Inviscid (potential) flow around circular cylinder



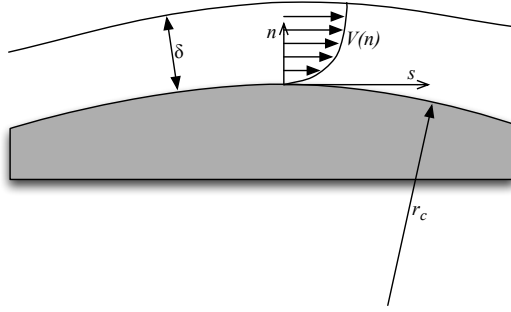
Viscous flow around circular cylinder

The inviscid flow is symmetrical and this means that the pressure along the front and the rear are equal, hence there is no drag. In contrast, the real flow is no longer symmetrical because there is a sizeable wake which is the result of separation at the sides of the cylinder. In the wake there is a relatively low pressure and this generates a large horizontal pressure force (because the pressure on the front and the rear of the cylinder do not balance) which is effectively drag.

We see here very clearly the cause of d'Alembert's paradox. The drag component generated by surface friction is indeed quite small. However the existence of viscosity can completely alter the flowfield and this in turn causes significant pressure drag. Without viscous effects there would be no flow separation and no low-pressure wake (and no drag). Although small, the effect of viscosity has significantly affected the flow.

Boundary layers

Let us consider a typical boundary layer on a randomly shaped surface in *steady* flow:



For simplicity, we are using a streamline coordinate system (this makes the equations simpler than the x-y-system used in the boundary layer part of 3A1). In this coordinate system the normal velocity $v_n = 0$ (this does NOT mean that wall-normal velocity is zero, because streamlines are not exactly parallel to the surface except for $y = 0$). The streamwise velocity v_s is equivalent to local flow velocity V ($v_s \equiv V$).

At the surface the velocity is zero to satisfy the no-slip condition. For most practical applications we can make a few general observations about the boundary layer flow:

Because Re is large, the boundary layer is relatively thin (its thickness is usually referred to as δ). This means that the local radius of surface curvature r_c is much larger than the boundary layer thickness (on a boundary layer length scale the surface is ‘flat’):

$$r_c \gg \delta$$

Since streamlines approximately follow the wall where we have large radii of curvature this indicates that the wall-normal component of acceleration is also negligible:

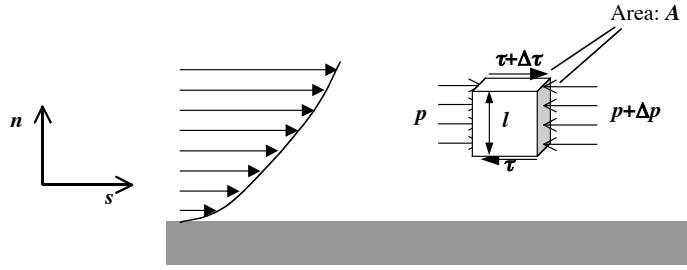
$$\rho \frac{V^2}{r_c} \approx 0$$

Furthermore, because we assume that there are no normal velocities, there is also no effective shear force in that direction. This means that in wall-normal direction the pressure forces alone balance the inertial force (acceleration) and since the latter vanishes we immediately conclude that there are no pressure gradients normal to the wall:

$$\frac{\partial p}{\partial n} = 0$$

This is a very important observation. It suggests that the pressure at the surface is equal to the pressure at the edge of the boundary layer. This assumption was first made by Prandtl when he introduced the concept of boundary layers. It implies that the pressure inside the boundary layer (and along the surface) is imposed by the outer flow and that it can be determined from a knowledge of the inviscid velocity field. At the boundary layer edge we may ignore viscosity and this means that we can use the Euler equations to determine the pressure field from the velocity field.

Inside the boundary layer we also need to consider viscous forces in the balance of forces on a fluid particle:



We proceed just as we did before by applying $F = m a$:

$$\begin{aligned} \text{Pressure Force + Shear Force} &= \rho Vol V \frac{\partial V}{\partial s} \\ -Vol \frac{\partial p}{\partial s} + \Delta\tau A &= \rho Vol V \frac{\partial V}{\partial s} \end{aligned}$$

For the shear stress we can use:

$$\tau = \mu \frac{\partial V}{\partial n}$$

and to estimate the change cross the element:

$$\Delta\tau = \frac{\partial\tau}{\partial n} l = \frac{\partial^2 V}{\partial n^2} l$$

so that we obtain:

$$\underbrace{-\frac{\partial p}{\partial s}}_{\text{pressure force}} + \underbrace{\mu \frac{\partial^2 V}{\partial n^2}}_{\text{viscous force}} = \underbrace{\rho V \frac{\partial V}{\partial s}}_{\text{momentum change}}$$

which is (almost) the boundary layer (momentum) equation as derived by Prandtl in 1903. Normally it is more common to use a wall-based co-ordinate system (x, y). In this case we can no longer assume that there is no velocity component in y direction which leads to an additional term on the right-hand side. For the purposes of obtaining a general understanding of the flow the above equation is useful because it describes the momentum balance along streamlines inside the boundary layer.

Note that we could replace the partial differential ∂p with the absolute dp because the pressure only varies in streamwise direction (which was the first boundary layer assumption).

The first term of the boundary layer momentum equation describes the force acting on a fluid particle due to pressure. This force is imposed by the outer inviscid flow and therefore depends only on the velocity distribution at the boundary layer edge.

The second term describes the viscous force. Generally the largest shear is experienced close to the wall. At the outer edge of the boundary layer the shear stress must vanish by definition (since viscous effects no longer matter here). Consequently boundary layer velocity profiles must have a vanishing gradient at the boundary layer edge often and generally (but not always) feature the largest velocity gradient near the wall.

$$\frac{\partial V}{\partial n} = 0 \quad \text{for } n = \delta$$

$$\frac{\partial V}{\partial n} > 0 \text{ for } n = 0 \text{ (except for reversed flow)}$$

This distribution of velocity gradients also means that the second term in the b-l momentum equation is likely to be negative.

$$\frac{\partial^2 V}{\partial n^2} < 0$$

In other words, the action of viscosity is to decelerate the flow inside the boundary layer (no surprises here). The effect of the pressure term depends on the sign of any pressure changes at the edge of the boundary layer – whether the outer flow is accelerating or decelerating.

The effect of pressure gradients on the velocity profile

First, let us consider the momentum along a streamline very close to the surface, deep inside the boundary layer. Here the flow velocity is close to zero (to satisfy the no-slip condition) and we can write approximately:

$$\mu \frac{\partial^2 V}{\partial n^2} \approx \frac{dp}{ds}$$

At the wall this relationship is exactly true:

$$\mu \frac{\partial^2 V}{\partial n^2} \Big|_{n=0} = \frac{dp}{ds}$$

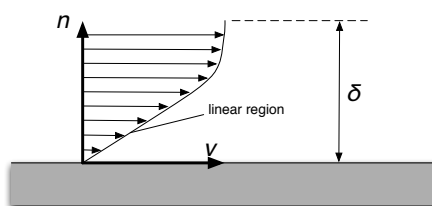
This shows that the second derivative of the boundary layer velocity profile near the wall (or exactly at the wall to be precise) is linked to the pressure gradient. The outer inviscid flow directly affects the viscous flow at the wall. Depending on the nature of the pressure gradient this has consequences for the shape of the boundary layer.

Uniform free stream

In cases where the velocity outside the boundary layer doesn't change (such as on a flat plate for example) the pressure inside the boundary layer is uniform. Therefore the second derivative of streamwise velocity vanishes (near the wall) and the velocity profile is linear near the surface:

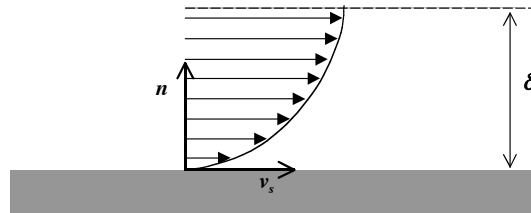
$$\mu \frac{\partial^2 V}{\partial n^2} \Big|_{y \rightarrow 0} = 0$$

(where y is the distance from the surface).



Favourable pressure gradients (accelerating free stream)

In cases where the boundary layer edge velocity increases in streamwise direction it follows that $dp/ds < 0$. This results in a profile with is more filled out (and there is increased wall shear stress):

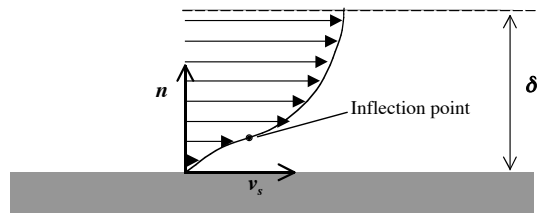


Adverse pressure gradients (decelerating flow)

In cases where the boundary layer edge velocity decreases we have a positive pressure gradient $dp/ds > 0$. This means that near the surface

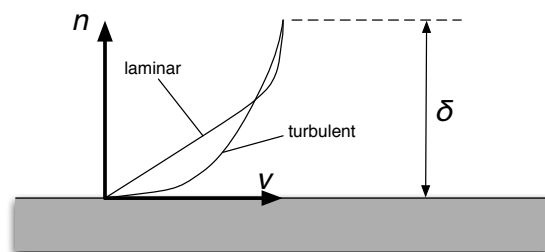
$$\mu \frac{\partial^2 V}{\partial n^2} \Big|_{y=0} > 0$$

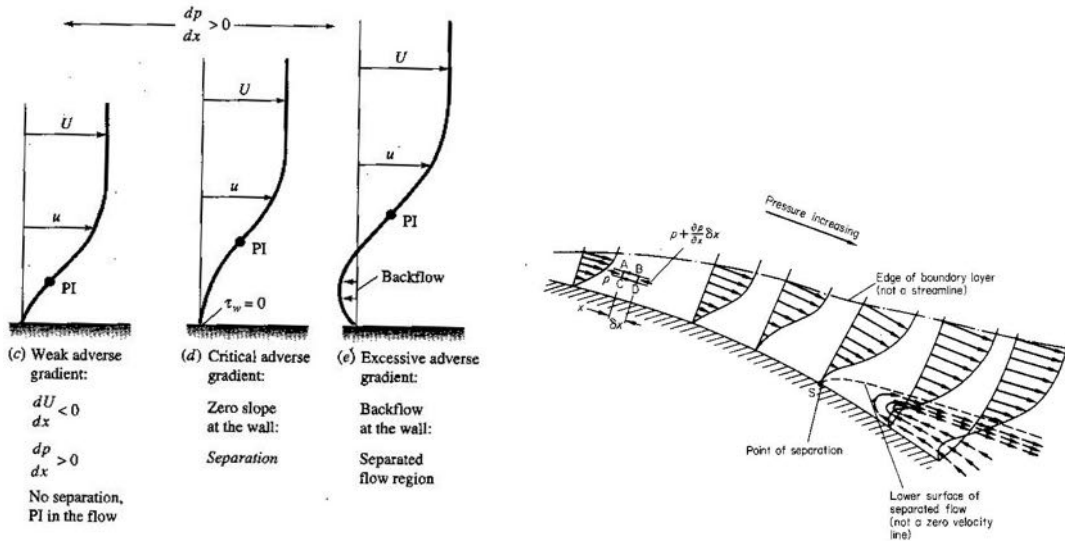
which is the opposite to the curvature of the profile further from the wall. Consequently, there must be an inflection point somewhere in the profile:



This shows that the near-wall flow is now decelerated quite strongly (more so than the outer flow) by the *combined* effects of friction and increasing pressure. Therefore, in a decelerating flow (where the pressure rises in streamwise direction) the change in momentum inside the boundary layer is even more negative than in the outer flow – a result of the ‘slowing down’ effect of friction. If such *adverse pressure gradients* are strong enough or persist for long enough the near wall fluid moves backwards. In this case the boundary layer has separated.

Turbulent boundary layers feature a fuller profile and are much more resistant to separation. Therefore, flow separation can sometimes be ‘fixed’ by forcing the boundary layer to become turbulent ahead of the adverse pressure gradient. This, of course, only works if the original separation was laminar.





The onset of separation from: a) White¹, b) Houghton&Carpenter²

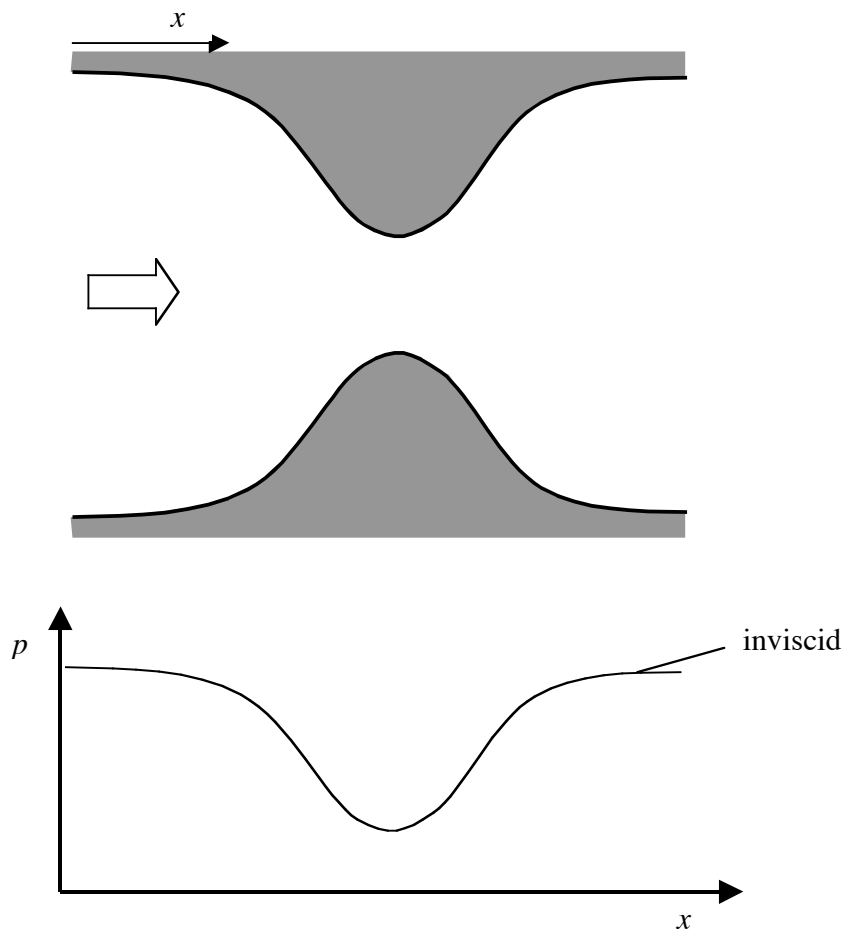
We see that flow separation occurs when the outer flow decelerates, generating an adverse pressure gradient. Flow separation can significantly change the overall flow pattern (in which case the region of viscous flow is no longer limited to a thin layer above the surface). To determine whether there is any danger of flow separation we can consider the inviscid flow and identify regions where adverse pressure gradients occur.

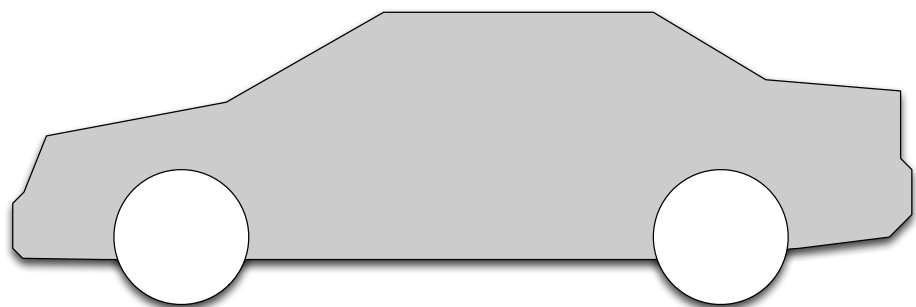
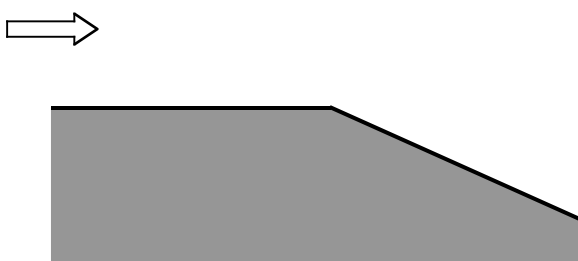
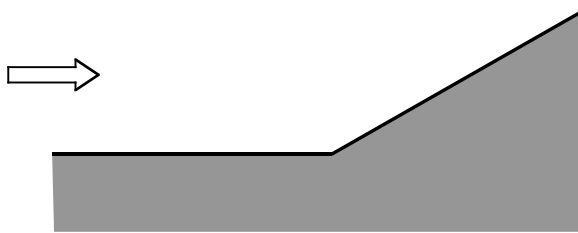
Pressure distribution in separated regions

Because the flow velocities inside separated regions tend to be much slower than outside, there are generally no significant pressure variations in separated regions. Often separations can be identified by surface pressure distributions that have gone ‘flat’ that is there are areas of relatively constant pressure where adverse pressure gradients would be expected if there was an attached/inviscid flow. The pressure inside the separated regions is often quite close to that at the separation point. Of course, these are just rough guidelines and the exceptions very much prove the rule.

We see that, once separation is encountered, viscosity can indeed have a significant effect, even on the inviscid flow.

Examples:



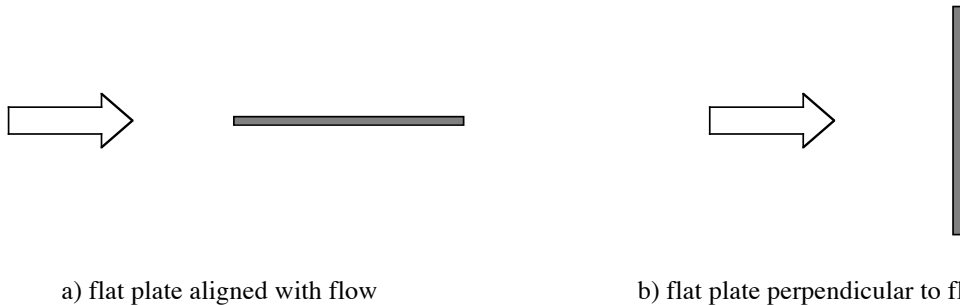


Drag of objects immersed in a flow

Pressure drag vs. skin friction drag

We have seen that viscosity causes drag in two ways, directly and indirectly. First of all there is surface shear stress which can be integrated to give an overall drag contribution termed *friction drag*. On the other hand, the presence of boundary layers is also responsible for flow separation and this often causes regions of low pressure, particularly at the rear of objects, and thus gives rise to *pressure drag*. Sometimes the latter component is erroneously thought of as an inviscid drag mechanism, but in incompressible flow this is clearly wrong – if flows were inviscid there would be no drag, neither friction drag nor pressure drag. Pressure drag is just another consequence of friction, although this is not always obvious.

To what extent the overall drag of an object is made up from friction or pressure drag depends very much on its shape. The flow around a flat plate (a) aligned with and (b) perpendicular to the oncoming flow is a good example for the two extremes:



For a flat plate aligned with the flow we can estimate the friction drag by using either Blasius' equations (if the flow is laminar) or an equivalent turbulent expression which is more appropriate in most technical flows. A good estimate for turbulent skin friction is obtained by assuming a boundary-layer profile in the shape of a 7th power curve, which gives:

$$\delta_2 = \frac{0.037 x}{Re_x^{1/5}} \quad \text{note: } \delta_2 \equiv \theta$$

$$c_f = \frac{0.06}{Re_x^{1/5}}$$

$$C_F = \frac{0.074}{Re_L^{1/5}}$$

These formulae assume turbulent flow originating at the leading edge (no laminar portion). Experiments have shown that these formulas work relatively well up to Reynolds numbers of 10^7 . (Don't forget to multiply by 2 if calculating the drag of a flat plate to account for upper and lower surface).

For a flat plate perpendicular to the oncoming flow friction drag vanishes (if it is infinitely thin). Pressure drag, however is considerable. Assuming an average pressure on the front p_F and back p_B (the latter is called *base pressure*), the drag coefficient is:

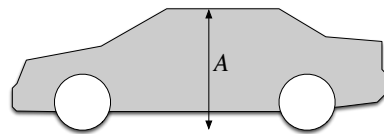
$$C_D = \frac{(p_F - p_B)A}{\frac{1}{2} \rho V^2 A} \approx O(1)$$

Bluff bodies are shapes where pressure drag dominates the overall drag (i.e. where there is a large wake).

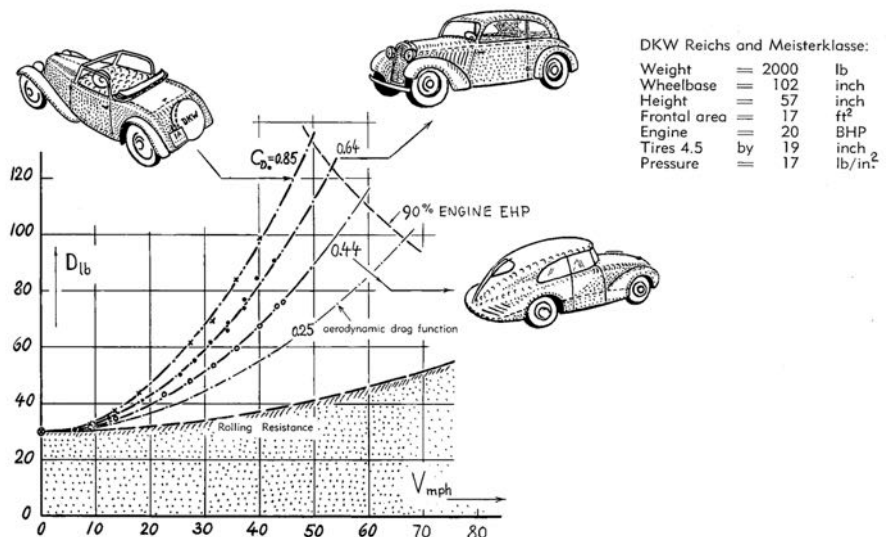
2. Introduction to Vehicle Aerodynamics

The drag of objects is normally non-dimensionalised by using a typical area and the free stream *dynamic* pressure to give a drag coefficient:

$$c_d = \frac{D}{A \frac{1}{2} \rho v^2}$$



Note that the conventions differ between fields. In aircraft the reference area is generally the wing area. Friction drag coefficients are sometimes calculated using the wetted area. In the car industry it is common to use the frontal (horizontally projected) area of a car as reference. Below is a very old picture comparing the relative contributions of rolling resistance and aerodynamic drag. Since then things have changed but while both rolling resistance and aerodynamic shaping have improved considerably, the relative importance of these two drag components has remained similar. This shows that for a reasonably well designed car ($c_d \approx 0.3$) aerodynamic drag begins to dominate at motorway speeds.



Drag of various car shapes from Hoerner³. Although car shapes have changed dramatically, the balance of aerodynamic and mechanical drag has not really altered (mechanical drag has also improved).

Basic flowfield

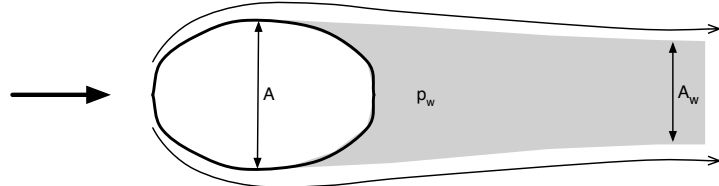
At a first glance, the most obvious problem is that typical road cars generally feature a large region of separated flow at the rear. Thus, cars are bluff bodies in the aerodynamic sense and their drag is dominated by the large separation and low pressure at the rear (base pressure). The reduction of pressure drag is therefore the foremost aim of vehicle aerodynamics.



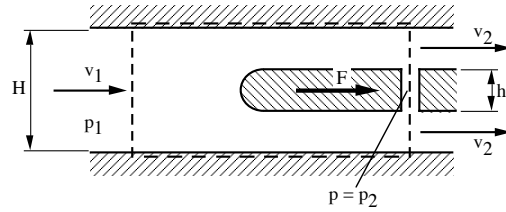
Flow over typical car shapes*

Bluff Body Drag

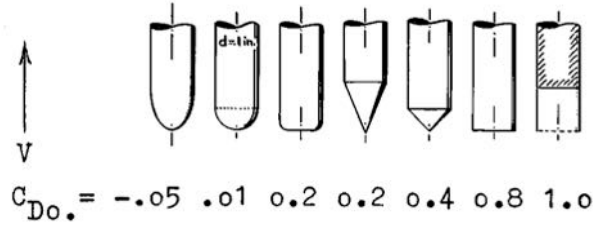
We can make a very simple argument to show the relationship between drag, separation size and base pressure. Imagine a randomly shaped bluff body with extensive separation at the rear:



From the 1A lectures you may recall that for the problem shown below the force over the front half of the body vanished for $H \gg h$.



In practice this is quite correct – a reasonably well shaped front end (which avoids separation) has very little drag (even negative drag is possible):



Drag coefficient of various nose shapes³

Returning to our example (and neglecting friction drag), vanishing forebody drag is equivalent to saying that the *average* pressure across the upstream facing surface is equal to the free stream pressure p_∞ . Inside the wake we can also assume constant pressure, the base pressure p_w . For the generic bluff body shown above this now means that the pressure drag force is approximately:

$$F = (p_\infty - p_w) A_w$$

(admittedly this is very crude, a proper momentum balance would be better)

* http://us1.webpublications.com.au/static/images/articles/i1086/108676_4mg.jpg
http://us1.webpublications.com.au/static/images/articles/i1086/108676_6mg.jpg
http://us1.webpublications.com.au/static/images/articles/i1086/108676_2mg.jpg

On bluff bodies base pressures in separated regions are typically below p_∞ (in contrast, the pressure at the trailing edge of a streamlined shape such as an aerofoil is usually above p_∞).

Expressing pressures and drag force in coefficients:

$$c_d = \frac{F}{\frac{1}{2}\rho V^2 A}$$

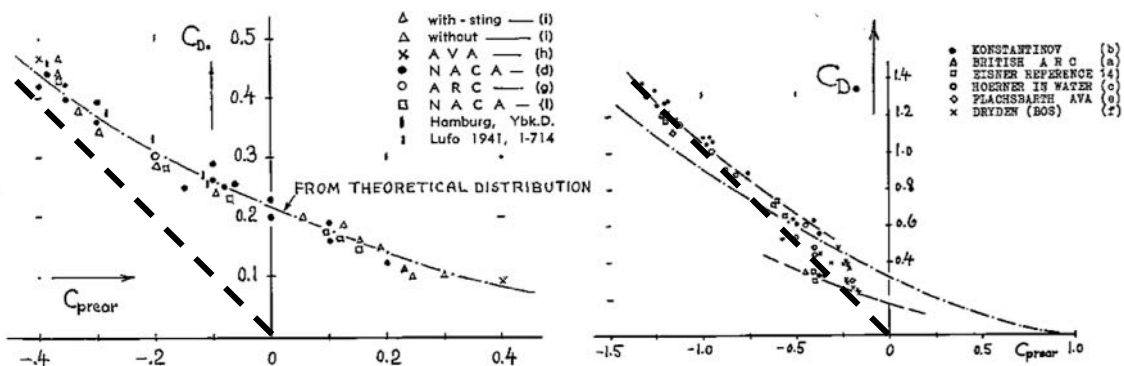
$$c_{p,w} = \frac{p_w - p_\infty}{\frac{1}{2}\rho V^2}$$

we obtain:

$$c_d = -c_{p,w} \frac{A_w}{A}$$

The above is obviously very rough but the link between base pressure and drag is well supported by measurements. The analysis suggests that there would be no pressure drag if the base pressure were equal to the free stream pressure. As a general rule, the pressure in the separated region is approximately equal to the pressure at the point of separation. In most cases the velocity at the separation point is greater than in the free stream – i.e. $c_p < 0$. A crude estimate for a 2-dimensional flow with significant separation would be $c_p = -1$. In that case a wake of equal cross-sectional area as the object would give a drag coefficient of 1.

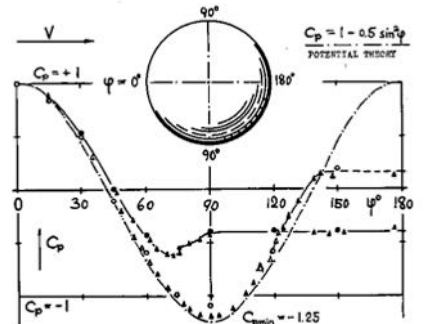
Below is some old data for circular cylinders and spheres comparing the drag coefficient with the base pressure coefficient. For the two-dimensional case the measured data follows the rough rule (indicated by the 45° dashed line) quite well, especially for large drag coefficients. However, the simple rule breaks down when base pressure coefficients approach zero (because the above equation would give a vanishing drag which is unrealistic). The agreement is less good for 3-d shapes, but once again, for large values of drag it is works well.



Link between base pressure coefficient and drag for spheres (left) and circular cylinders (right)³

The dashed diagonal lines indicates the expected drag coefficient following the simple analysis (assuming $A_w \approx A$)

Below is another example for a sphere with laminar and turbulent separation:

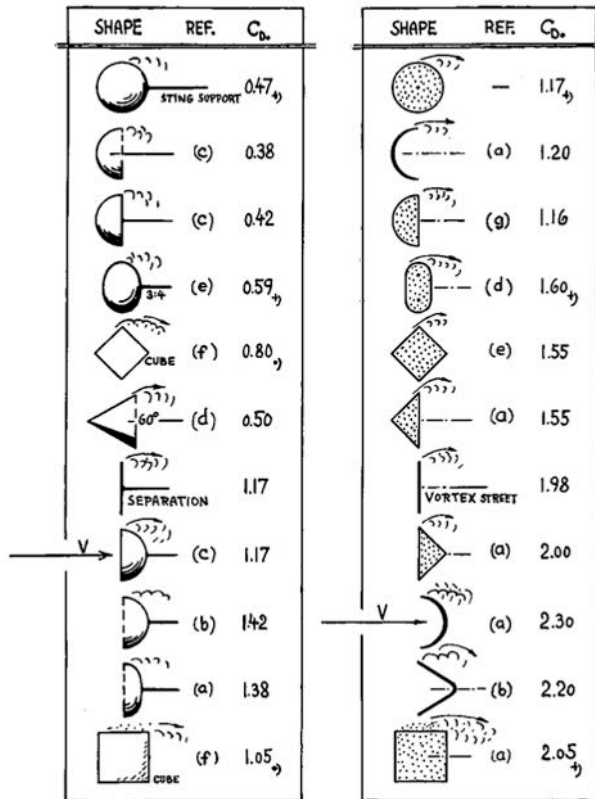


- AVA (16,h) AT $R_d = 1.7 \cdot 10^5$; $C_{D_*} = 0.45$
- DITTO, BUT AT $R_d = 4.6 \cdot 10^5$; $C_{D_*} = 0.09$
- ▲ ARC (16,g) AT $R_d = 1.6 \cdot 10^5$; $C_{D_*} = 0.47$
- △ DITTO, BUT AT $R_d = 4.2 \cdot 10^5$; $C_{D_*} = 0.14$

Pressure coefficients for spheres with laminar and turbulent flow³

In the laminar case, the base pressure coefficient is of the order of -0.45 and the drag coefficient is measured at 0.47 which is remarkably close to the approximate equation (assuming the wake cross-section to be equal to the sphere diameter). However, in the turbulent case the base pressure coefficient is slightly positive and the simple rule breaks down.

The main purpose of this analysis is that it allows us to estimate drag coefficients for bluff bodies with large separation (laminar spheres for example) and that it highlights the significance of wake area and base pressure. To get a feel for bluff body drag compare the data below for various 2-D and 3-D bodies. Note that in 2-D the drag coefficient c_D is roughly equivalent to the size of the wake (non-dimensionalised by body diameter). Hence, if the wake is larger than the body $c_D > 1$ and vice versa. For 3-D shapes we can see that $c_D \approx 0.45$ if the wake cross section similar to the body.

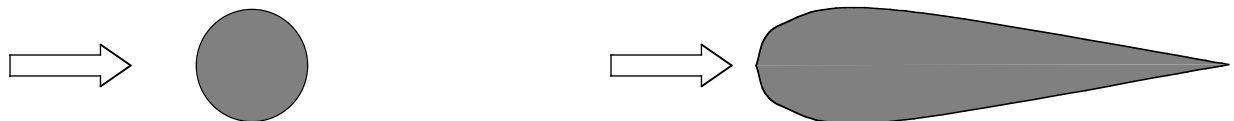


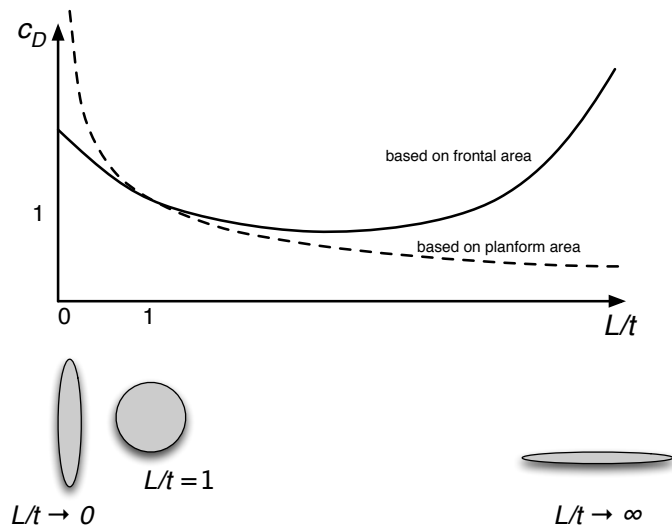
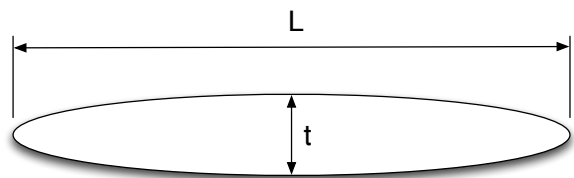
Drag of bluff bodies (left: 3-dimensional, right: 2-dimensional)³

Ultimately, the drag of bluff bodies can be reduced by either increasing the base pressure or reducing the size of the separated wake. Thus, the main aim is to delay the separation at the rear (because this reduces the wake size but can also increase the pressure at separation and thus the base pressure). The optimum is to avoid separation altogether – which leads us to the streamlined shape of the typical aerofoil. Here, there is no pressure drag but the increase in wetted area causes enhanced friction drag. Nevertheless, as we can see below, fully streamlined shapes have much lower drag coefficients than bluff bodies.

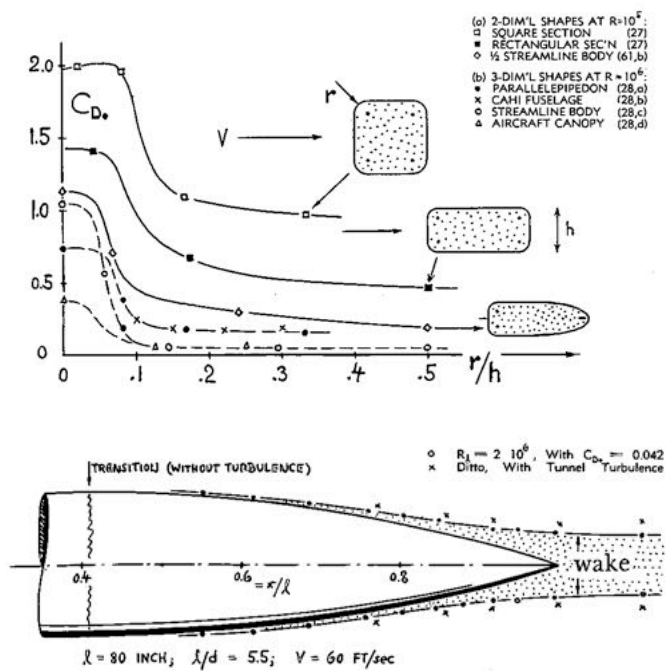
Streamlining

To achieve a reduction/delay of separation one needs to reduce the adverse pressure gradients. This generally results in more smooth shapes and the process is often called ‘streamlining’. Typically this is achieved by lengthening the object – especially at the rear where the adverse pressure gradients are experienced. With this approach the contribution of pressure drag can be reduced until friction dominates.





Drag of an elliptical body as a function of slenderness ratio



Reduction of drag coefficient by 'streamlining' (reducing wake size)³

3. Aerodynamic Design of Road Vehicles

Friction/parasite drag

The drag coefficient for a modern car is around 0.3, whereas the friction drag coefficient (using surface area) is only about 0.005. When taking the difference in reference area into account the contribution of friction can be seen to amount to about 10% of the total (I'm guessing a bit here...).

Therefore, most efforts in car aerodynamics concentrate on base drag but it is still worthwhile to pay attention to friction drag. On road vehicles it is unlikely that large regions of laminar flow can be obtained (because small surface details remain and insects and other dirt are likely to cause transition tripping). Therefore the only way to reduce friction drag is by reducing wetted area and minimising roughness (through improved surface finish or by eradicating ridges etc). A comparison of modern passenger cars with older models shows how much has been achieved through modern manufacturing methods.

Since attempts to reduce skin friction drag have in the past been limited by manufacturing technology most of the effort to reduce vehicle drag has historically concentrated on pressure drag.

Streamlined Cars

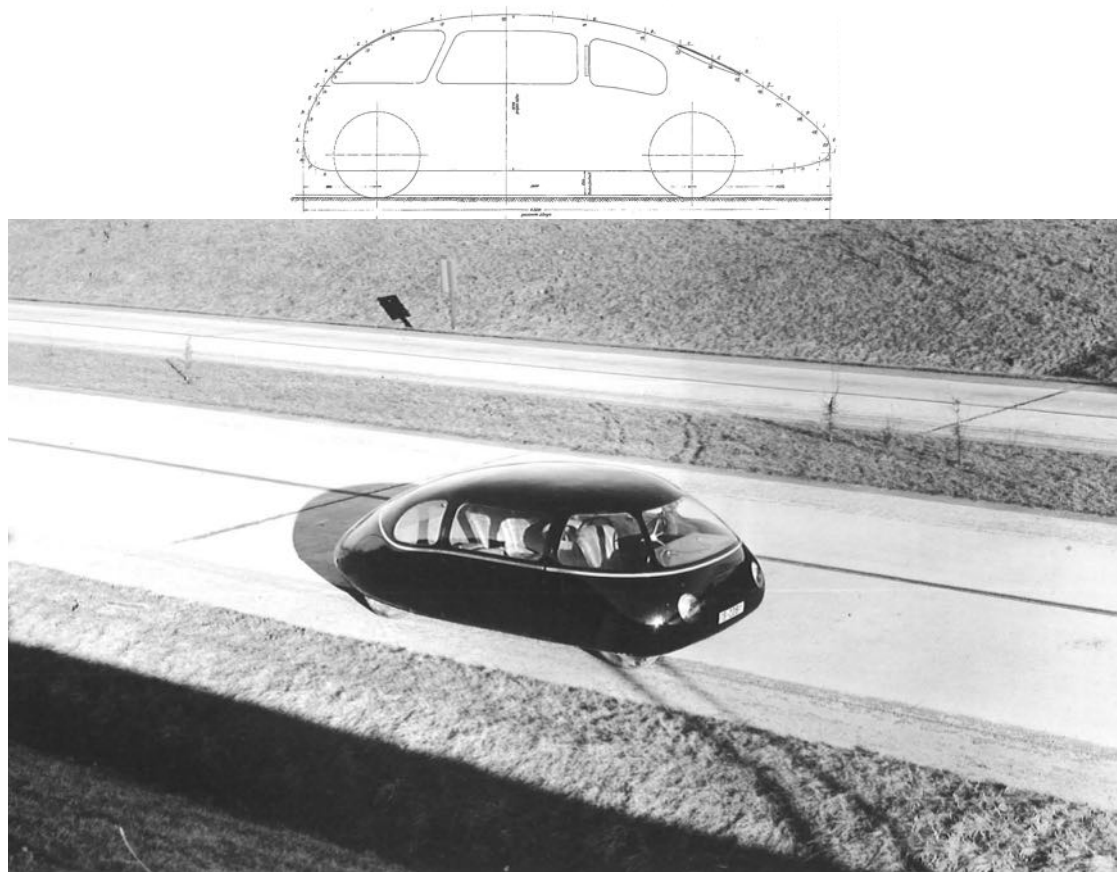
The desire to eliminate bluff body drag has led car designers towards fully streamlined aerofoil shapes. The most famous example is the 1924 ‘Tropfenwagen’ (‘droplet-shaped car’) by Rumpler which was tested by VW in 1983. Despite its ancient manufacturing technique, causing plenty of ridges and steps, it achieved a drag coefficient of 0.28 which most modern vehicles struggle to match.



Rumpler's *Tropfenwagen* (as seen in the *Deutsches Museum*, Munich)

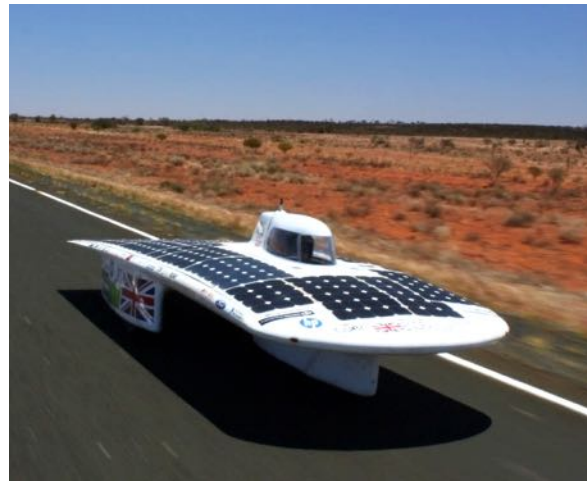


Rumpler's *Tropfenwagen* (as seen in the *Deutsches Museum*, Munich)



Concept car by Schlör ($c_d \approx 0.19$)[†]

[†] Der AVA-Versuchswagen, AVA report 43/W/26, Aerodynamische Versuchsanstalt Göttingen, 1943



CUER's Endeavour

Since then there have been further attempts at building aerofoil-shaped cars, although nowadays this design concept is limited to specialist vehicles. This is because streamlined cars are generally quite impractical. Interior space is not used very efficiently and they tend to be too long. Complex, curved shapes are expensive to manufacture and they suffer from poor cross-wind stability. This is because the centre of pressure (effectively the location where the lift vector acts) on aerofoils is at the quarter chord point and this is generally well ahead of the Cg of a vehicle. Thus, cross wind causes a destabilising moment. For this reason some streamlined vehicles feature large stabilising fins.



Streamlined motorbike with large stabilising fin

Practical cars

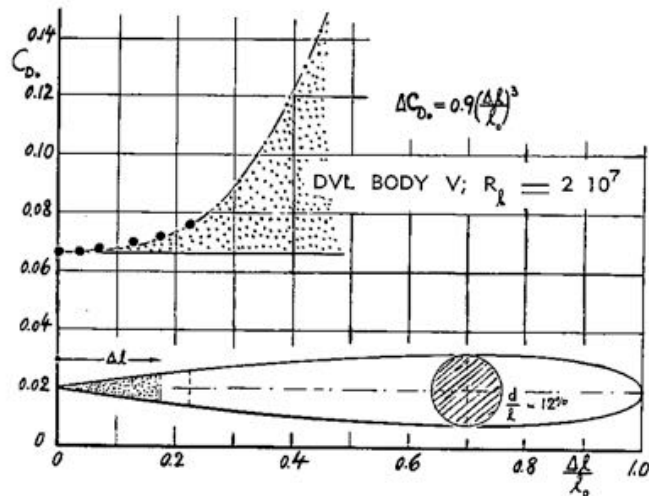
Because fully streamlined vehicles are impractical and difficult/expensive to manufacture much of the recent development has focussed on finding ways to reduce base drag within realistic limitations on overall vehicle length. The idea is to make the rear more streamlined while at the same time stopping well short of an aerofoil shape. Even small improvements to the flow at the rear of a bluff body can give considerable improvements if they delay flow separation. That is because any delay of separation has two beneficial effects:

- It reduces wake size
- It allows for a degree of pressure recovery, thus increasing base pressure

(Recall that drag is primarily determined by base pressure and wake cross-sectional area.)

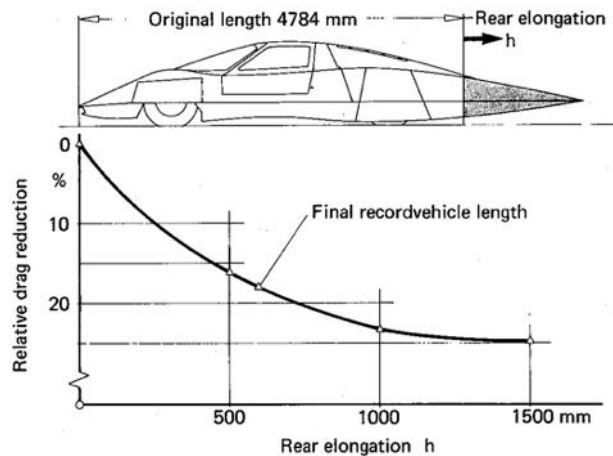
Boat-tailing

Experiments have shown that cutting off some of the trailing edge of a fully streamlined shape does not immediately cause a large increase in drag:



Effect of boat-tailing on a streamlined body³

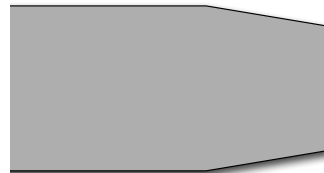
Similar results were obtained on a Mercedes concept vehicle:



Tail length study on Mercedes concept car⁴

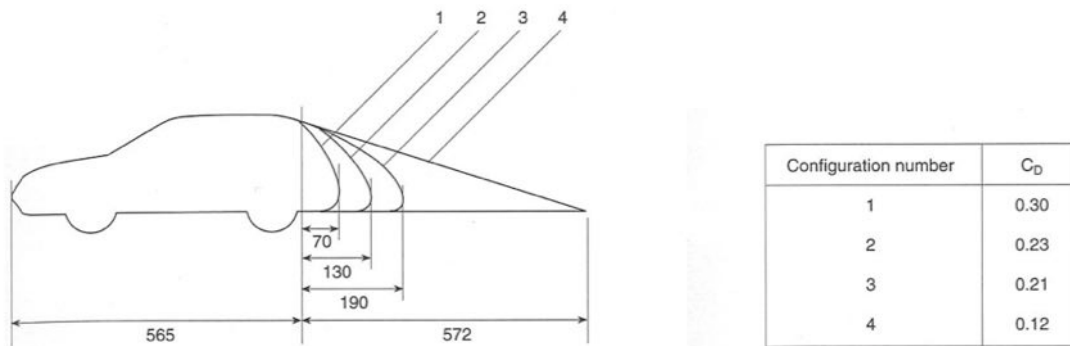


straight back



with boat-tail

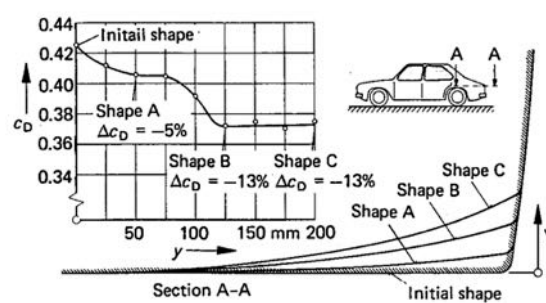
While the amount of rear shaping on the above example would still be impractical on a consumer car, these observations have led to the idea of 'boat-tailing' - adding a region of reducing cross-section at the rear of a bluff body. This reduces wake area and increases base pressure (due to some beneficial streamline curvature). Boat-tailing can achieve impressive drag reductions. However, it is important that the area reduction at the back is not too drastic (which might otherwise cause separation).



Effect of tail shape on drag coefficient⁵

In this above example, we see that somewhere between shape 1 and 2 a large reduction in drag is achieved. This suggests that shape 1 has a large wake, i.e. the flow separates at the roofline, whereas shape 2 manages to keep the flow attached for considerably longer (with little additional body length, compared to the fully streamlined shape 4).

More potential for boat-tailing can be found on the sides of a car:



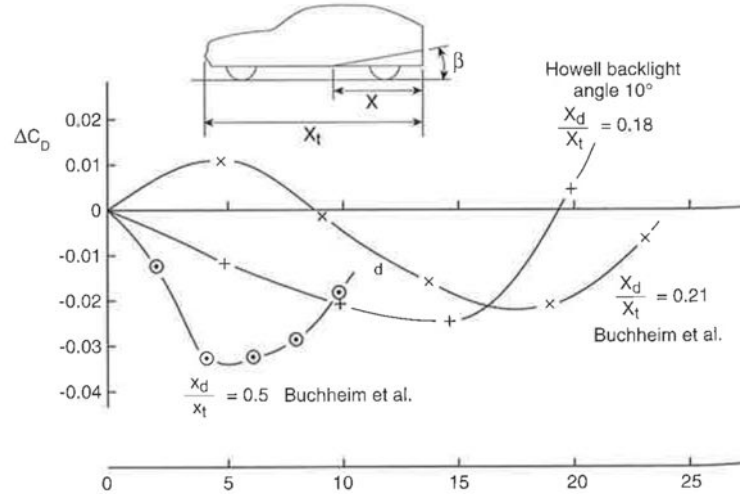
Effect of boat-tailing the sides of a car⁶

This is a very common approach as seen here on a Mercedes coupe:



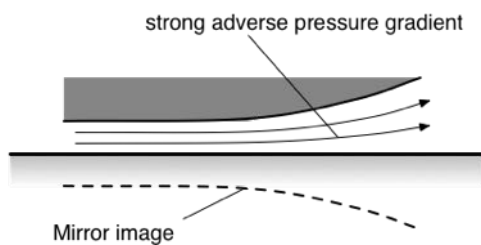
Mercedes coupe (rear)

A similar approach works for the underbody:



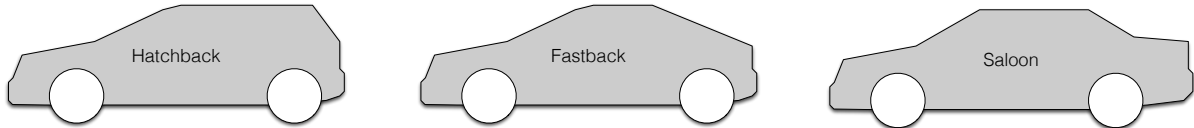
Effect of underbody boat-tailing (adding a rear diffuser)⁵

However, when considering underbody flow the presence of the ground becomes important. There is a danger that the increase in area for the underbody flow between the middle of the car and the rear can be too extreme. This is because the presence of the solid ground surface makes this effectively a diffuser flow which can be prone to separation if the area change is too aggressive. This is the reason for the pronounced maxima in the drag savings followed by a sharp drop when the optimum angle is exceeded.



The Effect of Tail Shape on Drag

The rear of most cars falls into three categories, *hatchback* (sometimes called *squareback*), *saloon* (or *sedan* in US English) and *fastback*:

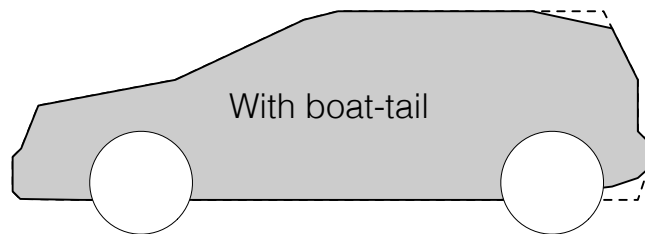


Basic car shapes: Hatchback, Fastback and Saloon

From an aerodynamicist's point of view all of the above are *bluff* bodies and thus the main drag contribution is the size (and pressure) of the wake. Hence, the key question is where the flow will separate on either shape.

Hatchbacks

In the hatchback it is obvious that separation is at the top of the rear window – thus there is a relatively large wake. However, most modern designs manage to improve matters considerably by introducing a small amount of boat-tailing:

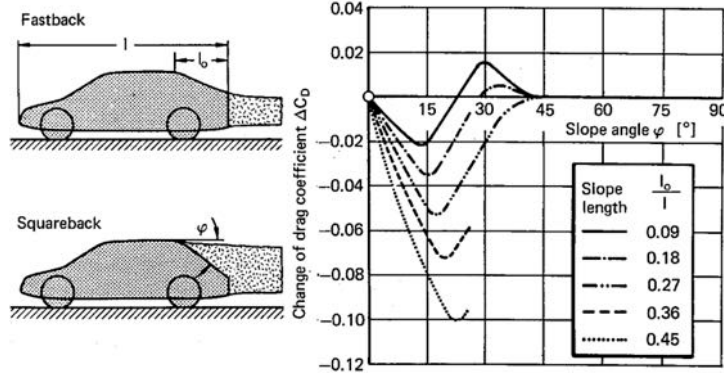


Boat-tailing on a hatchback shape (keep in mind that the sides can also be boat-tailed)

Although the boat-tailing on hatchbacks is quite subtle (to avoid losing too much interior space) the reduction in base area can be quite considerable (have a look at modern hatchbacks in the car park and compare their base area with the maximum cross-sectional area in the passenger compartment). The improvements in the drag coefficients of hatchbacks in recent years have been quite impressive with very little obvious change in shape (the first Golf reputedly had a drag coefficient of 0.42, the most recent version is nearer 0.31).

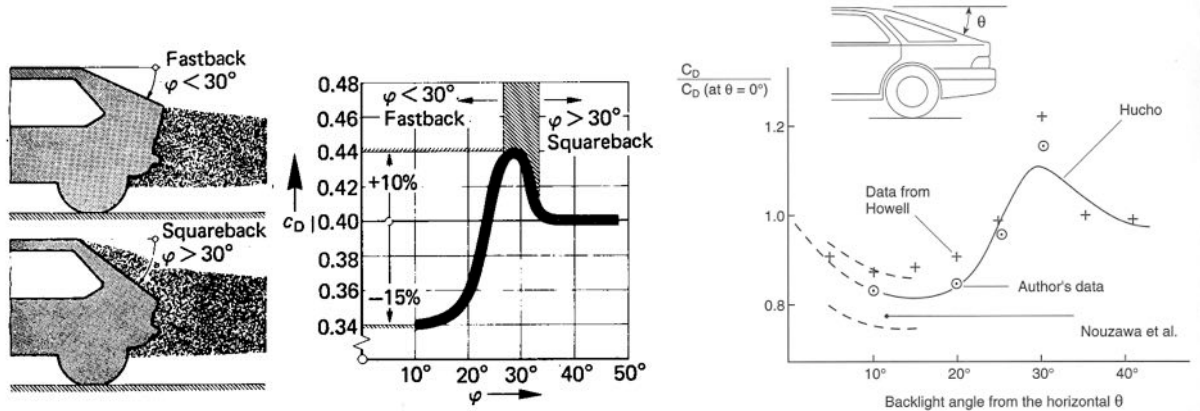
From Hatchback to Fastback

For saloons and fastbacks the location of the separation point at the top is less obvious. To produce a small wake (and thus reduce drag), it would be desirable to maintain attached flow onto the rear of the boot lid. Whether this can be achieved depends primarily on the slope ('*sweep*') of the rear window. Many studies have shown that attached flow is achievable for slope angles up to 30° , beyond which the flow separates at the roof line:



Effect of rear window slope on wake and drag⁴

As we see in the further examples below, drag reduces quickly for sweep angles below 30°. However, to reduce the wake size, smaller slope angles also require more length (which is difficult for small vehicles where it adversely impacts internal volume). A good practical target is around 20°. At this angle the flow should be attached all the way to the rear which gives considerable drag savings – and this is effectively the definition of a ‘fastback’.



Effect of rear window slope on drag^{7,5}

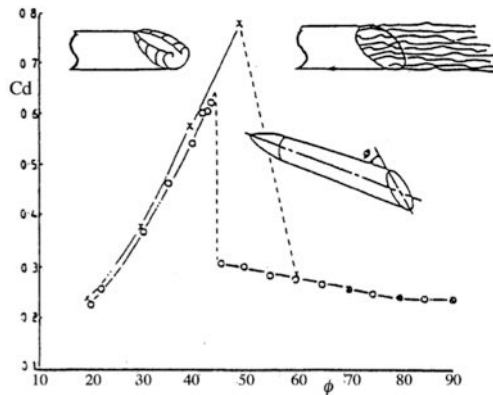
For small cars where the maximum length is limited a shallow rear slope can cause problems because the rear corner is very high – in the line of vision. Sometimes this is tackled by extending the glass onto the vertical section of the car as seen in the Honda Civic:



Larger cars can more easily accommodate a long section of low-ish slope angles, giving the classic fastback shape:



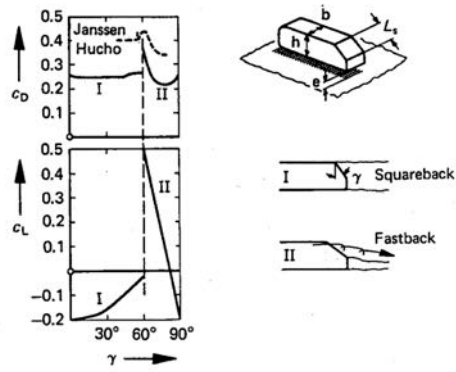
Summing up, we can expect attached flow (and thus lower drag) for slope angles below 30° and separated flow for steeper angles (which is the hatchback regime). However, this does not explain why there is a region of increased drag around the transition from one regime to the other. The cause of this is best illustrated by the simple study of the drag of a bluff body with varying rear slope performed by Bearman⁸:



Effect of rear cut-off angle on the drag of cylindrical bodies (Bearman⁹)

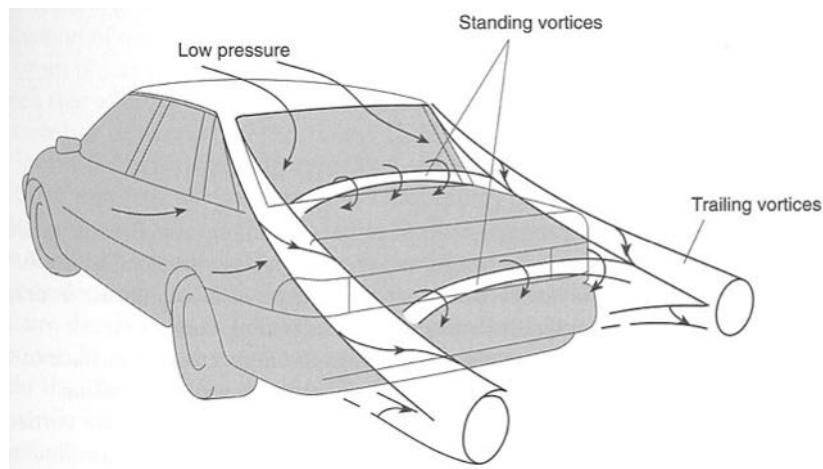
Here we see that the attached flow state generates higher drag coefficients than the bluff body flow with fully separated wake. The reason for this is that in the ‘attached flow’ state the sharp swept edges of the rear cause localised flow separation and the generation of vortices – just like on a delta wing. Depending on the body shape these vortices can be rather strong. Again, just like on the delta wing, the vortices introduce low pressure regions giving rise to additional lift and drag. In the above example this effect is more pronounced than on a car because the round cross-section of the body makes the edges even more swept relative to the flow. Nevertheless we can see that the vortex intensity (and thus the drag) increases with the sweep angle until the fully separated wake state is reached around 45° . However, it is also worth noting that at low sweep angles the drag of the swept section is less than that of the fully separated case (where sweep is $> 45^\circ$). And at 20° the drag is once again lower than a square cut-off.

Similar behaviour has been reported on square shapes, more relevant for vehicles:



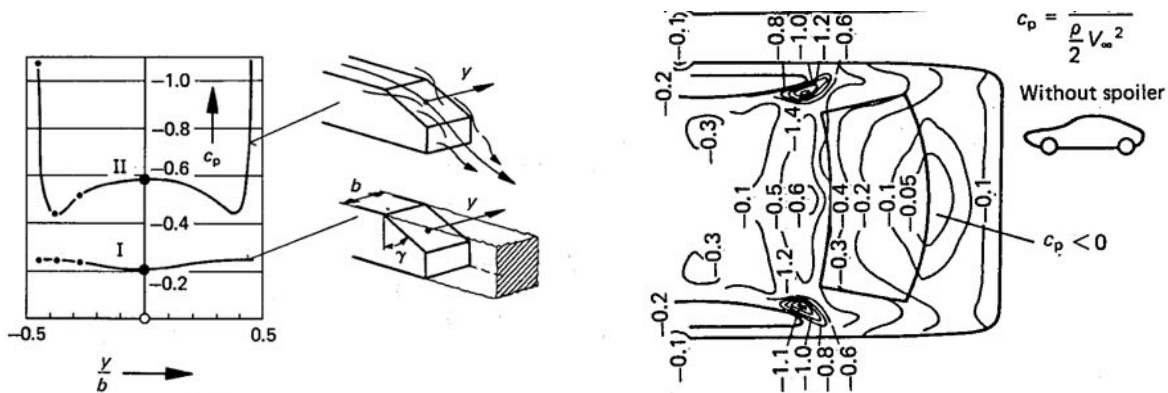
Various studies of drag with rear sweep angle, note the different definition of sweep angle (Conan et al.¹⁰)

On a realistic car shape the vortices sit near the outer edges of the rear window.



Vortices around the rear of a car (schematically)⁵

The vortical flow is seen clearly in flow visualisation and surface pressure plots. Below are examples from various studies:



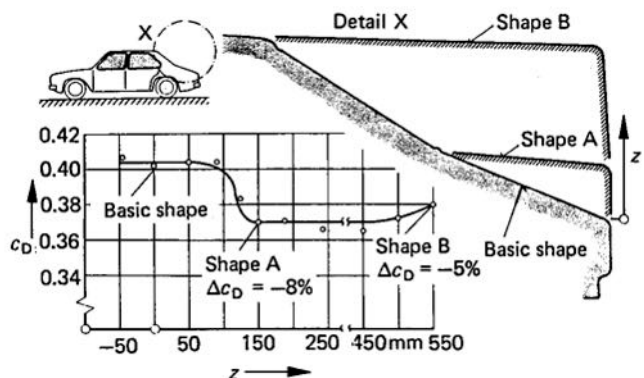
Various examples of vortical tail flows⁴

In the last examples the low pressure regions caused by the vortices are seen clearly – in contrast the more gradual pressure change along the centreline suggests attached flow there.

The low pressure caused by the vortices also contributes greatly to lift – and this effect remains up to very low sweep angles. This can be a problem for high performance cars where lift is undesirable.

Saloon shapes

Saloon cars are generally longer and have a classical boot lid with access from above. Below we see a study comparing the drag on all basic shapes (fastback, saloon, hatchback):

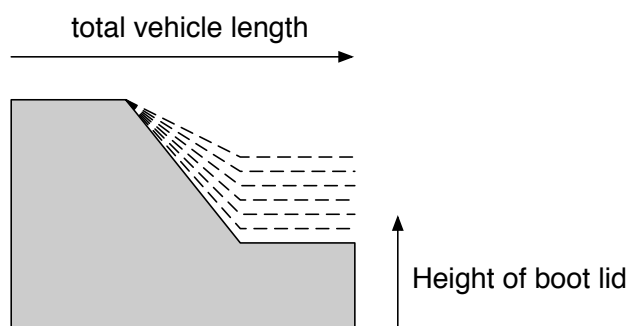


Comparison of basic tail shapes⁶

Here it is interesting to note that the ‘basic shape’ (fastback) has a higher drag than the saloon-type ‘shape A’. This unexpected result is probably due to a number of reasons:

1. The flow may not remain attached all the way to the trailing edge in the ‘basic shape’ – the adverse pressure gradient has gone on for too long (note also the position of the lower window ridge which may trigger an earlier separation)
2. The ‘basic shape’ may introduce strong vortices with an associated drag penalty. In fact, the sweep angle looks to be around 27° which is quite a bit steeper than 20° and would therefore be expected to suffer from significant vortex drag.

Ultimately flow visualisation would be needed to analyse this behaviour. Nevertheless, for the above car the most promising shape is some variant of the saloon (with a relatively short boot). Using the results seen earlier (for fastbacks) we would correctly assume that the rear window slope should be around 20° for optimum performance. Thus, a critical design parameter is often the height of the boot lid. By raising this, the angle of the sloped rear window can be decreased to get close to 20° . However, once the flow is attached all the way to the rear, raising the boot further results in greater wake area (unless the car is lengthened). Alternatively, the basic shape could be revisited by making it a less steep fastback shape which (if large vortices can be avoided) is likely to result in an even better performance (but there may be practical considerations against it (such as boot access etc)).

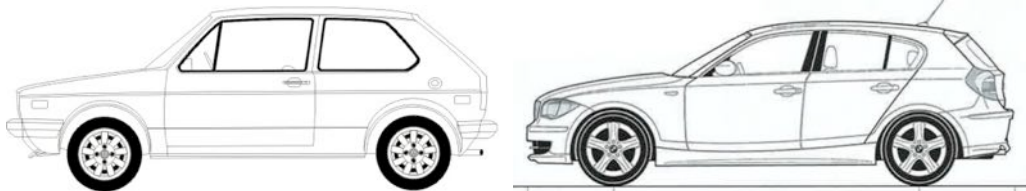


Raising the height of the boot lid reduces rear window slope
(but increases size of base area unless the car is lengthened)

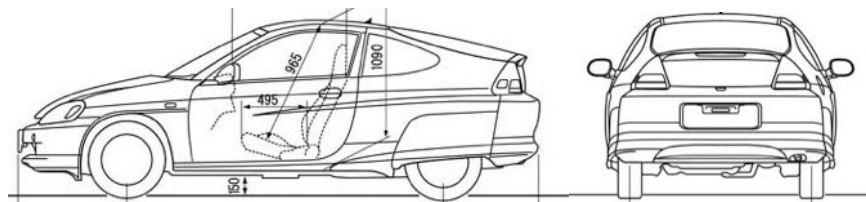
Summary

Very simplistically we can summarise the key flow features of the three basic shapes as follows:

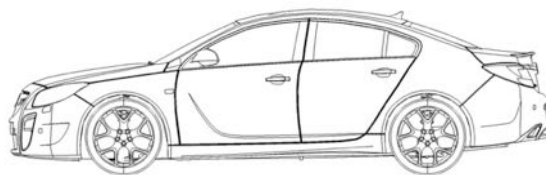
- Hatchback: Large separation (at the roof line) but maximum internal volume (good for short cars). In its most basic configuration (without any boat-tailing, think of the original Golf, left, original $c_D > 0.4^{\dagger}$) this has relatively high drag, but more modern shapes (BMW 1-series, right[§] – look out for the amount of boat-tailing, which is also significant on the (not seen) sides) can be very efficient (for the BMW: $c_D = 0.29$).



- Fastback: Attached flow along the rear window but possibly with strong vortices. Not good for volume (boot space) or access to the boot. There is a danger that significant lift is produced (and thus, strong vortices). If strong vortices and separation can be avoided (keeping the angle small, 15° - 20°) this shape has the most potential for minimum drag, see e.g. Honda Insight[†] ($c_D=0.25$) – which has significant boat-tailing on the sides as well as the top. See also Toyota Prius below. To reduce the size of the base area (and thus the wake area) it may be necessary to lengthen the car or start the slope earlier (which adversely affects internal volume).



- Saloon: These cars are generally larger (thus longer) which helps. Ideally, there is attached flow along rear window and the boot lid (which can be quite high to reduce the sweep angle). The separation point is at the rear of the boot lid. Can have vortices (but not as strong as fastback). Decent use of space through classical boot with easy access. Modern cars using this shape can have very low drag coefficients, approaching the best fastbacks (Vauxhall insignia[†], below, $c_D=0.26$ - 0.27 , sweep angle $\approx 20^{\circ}$).



It is interesting to note that the above three basic shapes are beginning to merge more and more as aerodynamic design has improved. With some cars it is hard to tell which category they fall in. Common to most is the attempt to reduce the area of the wake by introducing as much boat-tailing as possible without making the car too long. In practice this leads to boot lids relatively high above the floor. Keep in mind that it is not just about the roofline – the sides can be shaped aerodynamically as well (bringing the sides in at the rear). Although not obvious, most modern cars have significantly smaller area at the back (even hatchbacks) than their maximum cross-section area.

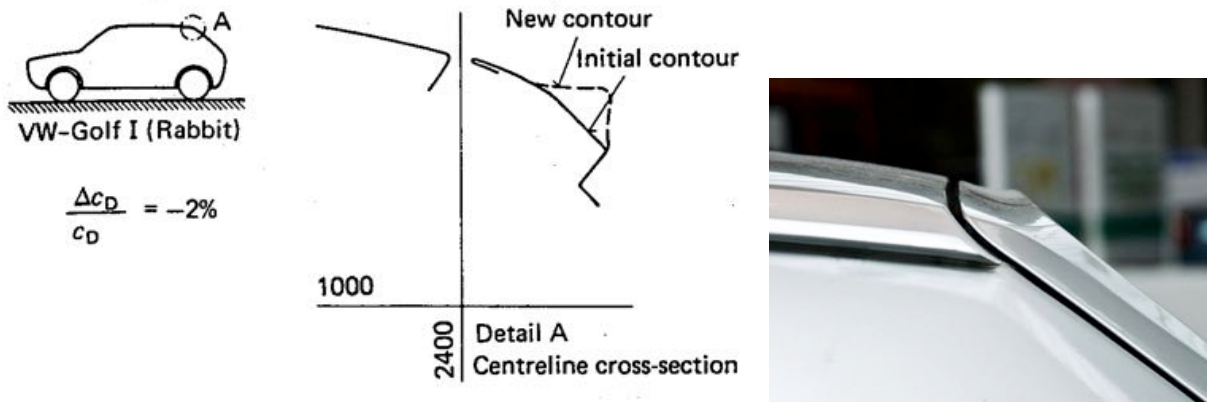
[†] Image from: <http://www.smcars.net>

[§] Image from BMW drivers manual

Details: Other Areas for Drag Reduction

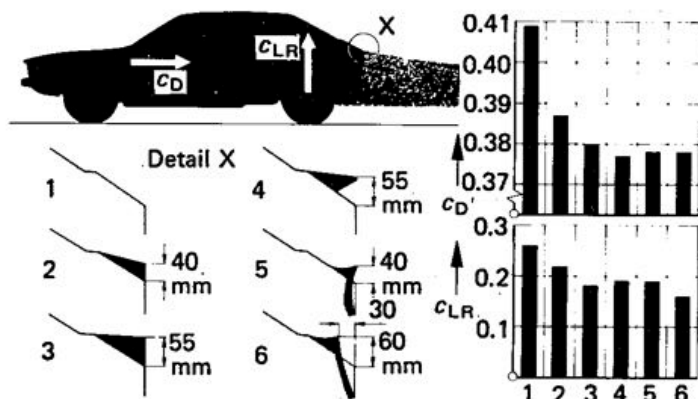
Rear detailing

In regions where we expect separation it is best to ‘fix’ this with a well defined edge as seen in the modifications made to the first VW Golf:



Effect of lip on hatchback drag⁴

Similarly, small separation lips can also reduce drag on fastback shapes:



Effect of small rear lip (spoiler) on drag⁴

To understand why these devices work, it is important to remember that base drag is the combination of wake area and base pressure. Small spoilers or modifications to the surface contour ahead of the corner slightly increase the wake cross-sectional area which is detrimental. However, they also introduce a little concave curvature to the streamlines just ahead of separation which increases the local pressure – and this in turn fixes the base pressure at a higher level. This can offset the increased base area to give a lower drag overall. Also, if the separation point is not clearly determined by the surface geometry (such as on a gently rounded shape) then it is likely that the location of separation fluctuates. This can cause undesirable unsteady flow and the average location of separation may be worse than that achieved with a fixed edge.

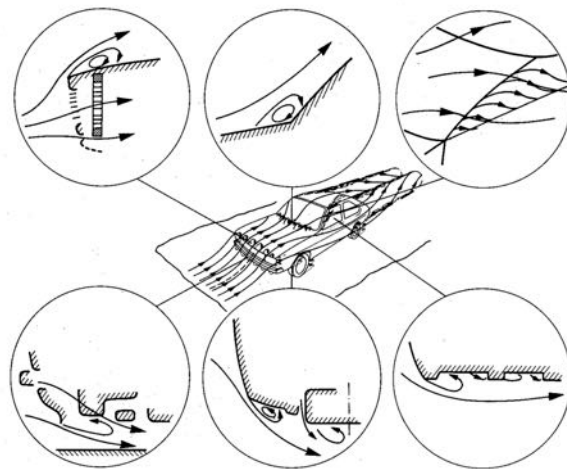
Nowadays it is rare to see any cars without a ‘lip’ just ahead of the separation point which suggests that the effect of increasing base pressure generally outweighs the increased wake size. The lesson appears to be that if separation can not be avoided it is best to start it with a well defined edge.



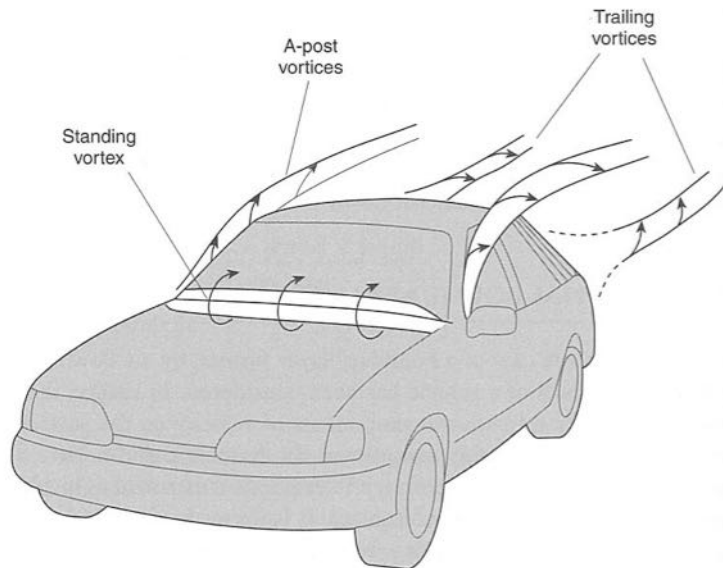
Small lip at rear of a saloon car

Front shape

Although the large wake at the rear is responsible for much of the aerodynamic drag, other areas also contribute. Surface roughness introduced by gaps between body panels and steps in the surface (e.g. around the windows) can increase the friction drag. Other features can cause localised flow separations.



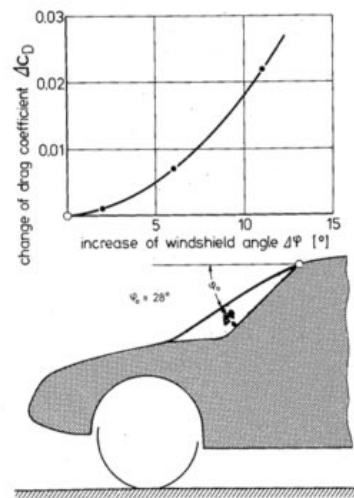
Typical flow separation regions on a car⁴



Vortices on a generic vehicle⁵

Particular problem areas are the front windshield where there can be a separation bubble at the bottom junction with the hood, the ‘A-pillars’ (‘A’ because they are the first pillars on a car – followed by ‘B’ and ‘C’ pillars) and the front edges.

The windshield separation bubble is affected by the slope of the windscreens and the smoothness of the transition from the bonnet (which is difficult to achieve because of the need for wipers, ventilation and seals). Obviously shallower angles are better (except for the increase in wetted area if the car gets longer), but shallow angles cause problems with the internal lay-out and experience more solar heating.



Effect of windshield angle on drag

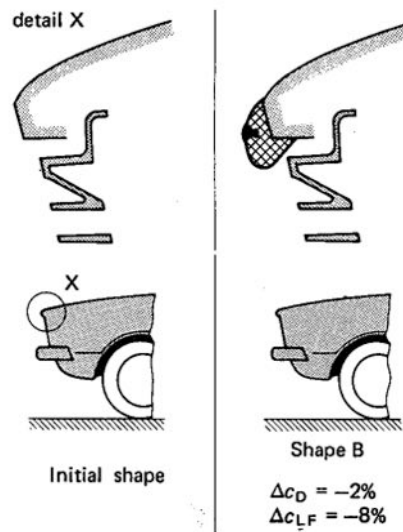
In modern cars the windshield is swept considerably and the separation bubble at the foot of the windshield does not contribute much to the drag (quite a contrast to old cars which had much steeper windshields). Nowadays the wipers can be a more significant source of parasitic drag. Many modern cars now have wipers hidden behind a deflector – confirming that the separation bubble is less of a problem than the wipers.



Windscreen wiper deflector

Separation across the A-pillars can be avoided by ensuring a smooth surface without steps and a sufficiently large radius of curvature. Modern production methods make this possible.

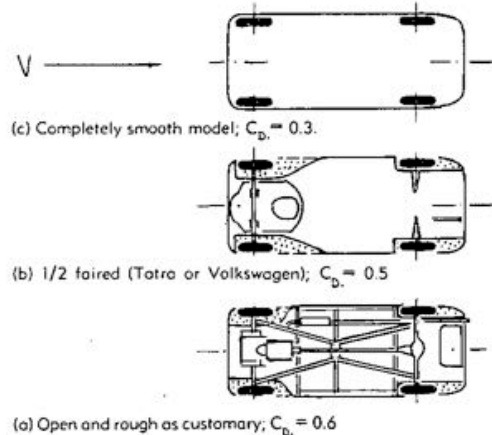
Similarly, separation on the hood is prevented by an aerodynamically smooth (and sufficiently rounded) nose shape:



Effect of front detail on drag⁴

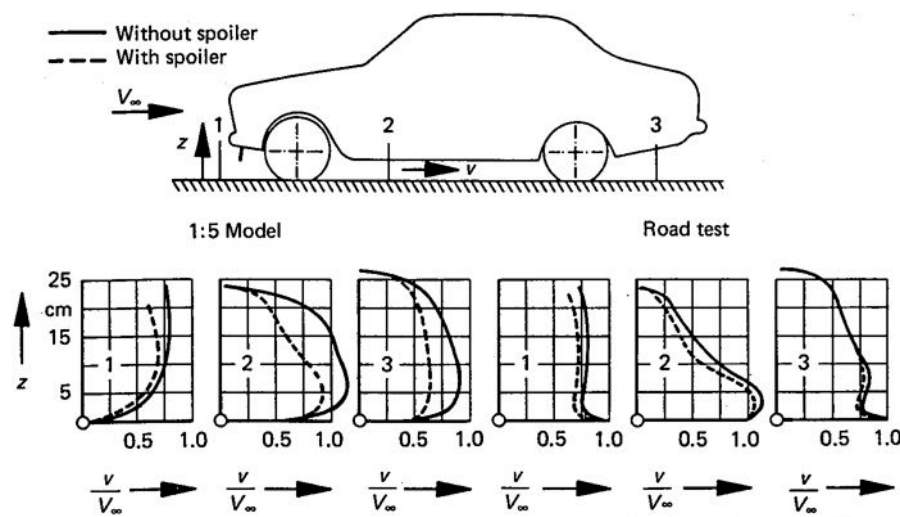
Underbody

A significant contribution to the drag of a vehicle is caused by the underbody flow. Unfortunately this is also the least streamlined area because access is needed to various mechanical components. An obvious solution would be to apply aerodynamic cladding but this complicates maintenance, might introduce overheating, and incurs additional cost. Since the average car buyer rarely inspects the underbody it is also not exactly a ‘sexy’ area for designers.



Effect of underbody roughness on drag³

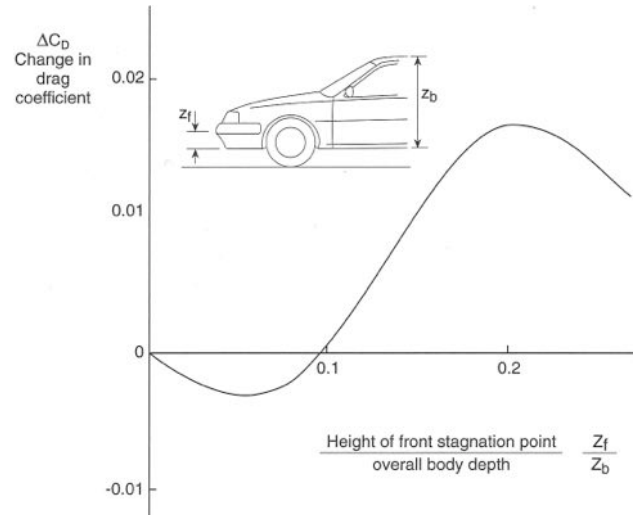
Given that a degree of ‘roughness’ is unavoidable underneath a car one way of reducing drag is to decrease the average flow speed in the underbody area. This can be achieved by restricting the flow entering at the front with a spoiler:



Effect of front spoiler on underbody flow⁴

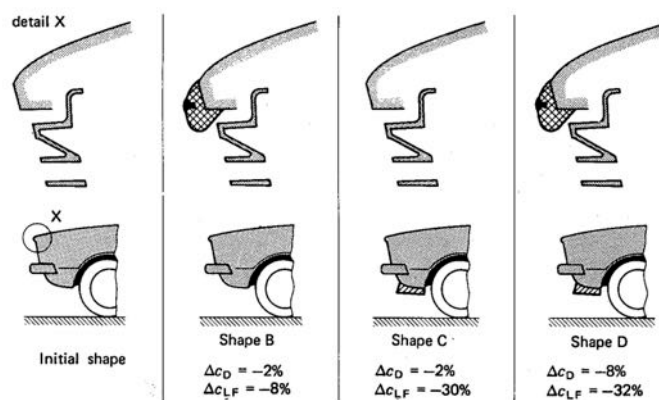
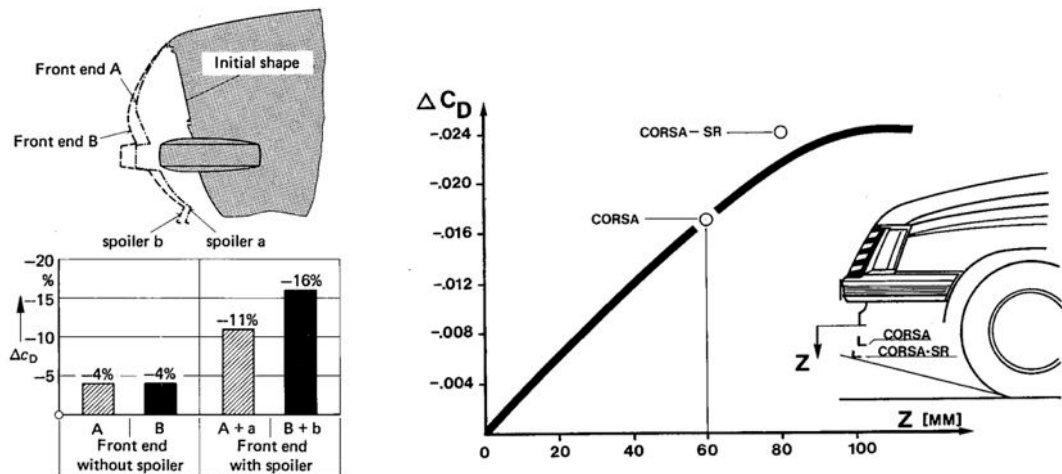
Nowadays front spoilers are an important part of the design of modern cars (although rarely noticed).

Another way of reducing the flow speeds underneath the car is to move the stagnation point at the front downwards (by careful design of the nose). This reduces the amount of flow underneath the car (more air is deflected above the vehicle). The effect on drag is comparable to placing a spoiler underneath the nose.



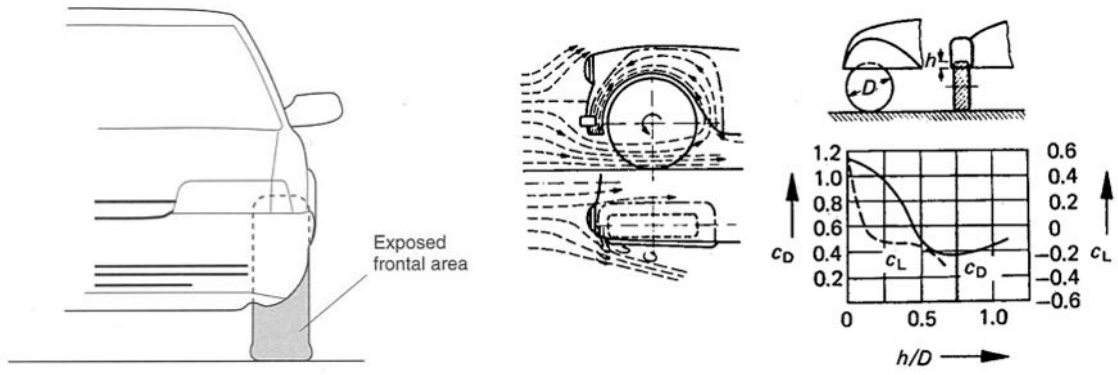
Effect of stagnation pressure position on drag⁵

Here are some other examples highlighting the drag savings achieved by front spoilers:



Front spoiler effect⁴

A further contribution to aerodynamic drag is the flow around the wheels:



Aerodynamic drag of wheels^{5,3}

Nevertheless, it is unavoidable that some of the wheel is exposed to the flow. The additional drag is proportional to the exposed area. This means that slimmer wheels produce lower overall drag. Standard cars will always be measured with their narrowest wheels (even if the brochures show the wider wheels for looks) and eco- or concept cars (designed for low drag) will always feature relatively narrow wheels (with the added advantage of reduced rolling resistance). Wheel drag can be reduced by protecting them from the flow through side skirts and, more commonly, small front spoilers underneath the car.

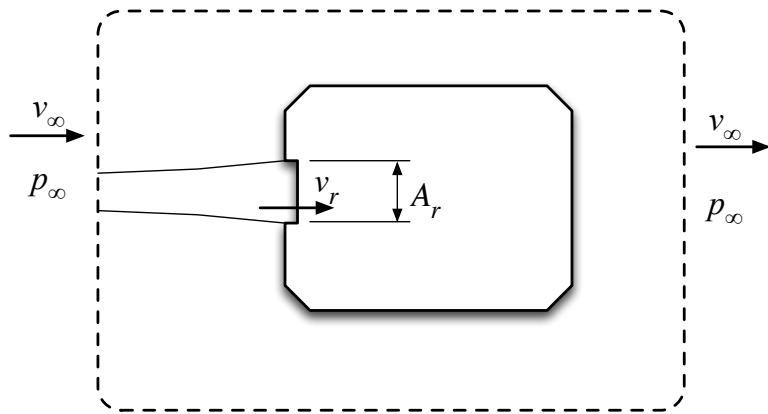


Small front spoiler ahead of wheel

Drag due to cooling flows (radiators)



The air entering the car through the radiator causes considerable additional drag. This is apparent if we take a control volume approach. Here we assume a radiator area A_r with a local flow velocity on entry v_r .



We can assume that the mass flow entering the car through the front radiator (which has a stagnation pressure equivalent to free stream) eventually leaves with negligible momentum (relative to the car). Thus, its momentum is 'lost' which causes drag. A momentum balance then provides the following additional cooling drag coefficient:

$$F = \dot{m}_r(\mathbf{0} - \mathbf{v}_\infty)$$

$$F = -\rho A_r v_r v_\infty$$

$$c_{D,r} = \frac{\rho A_r v_r v_\infty}{\frac{1}{2} \rho v_\infty^2 A} = 2 \frac{v_r}{v_\infty} \frac{A_r}{A}$$

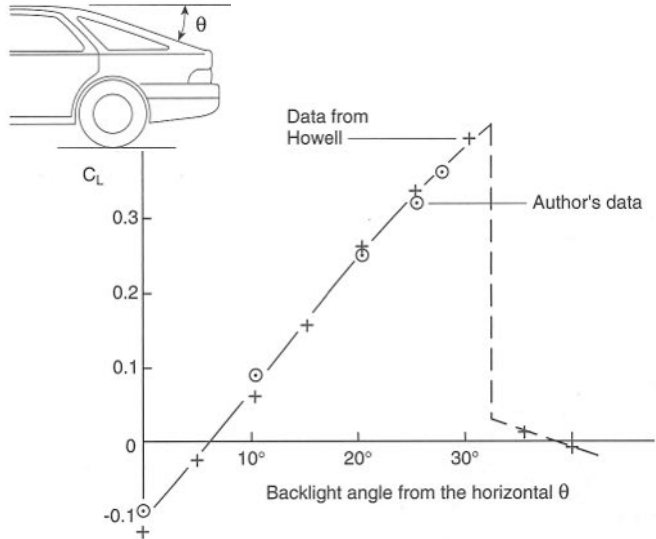
or

$$c_{D,r} = \frac{2 \dot{m}_r}{\rho v_\infty A}$$

where A is the cross-sectional area of the car. Thus, to reduce radiator drag the mass flow and radiator area should be kept as small as possible. Also, it is helpful to place the radiator in the region of the expected stagnation point as this will help the flow to pass through the system.

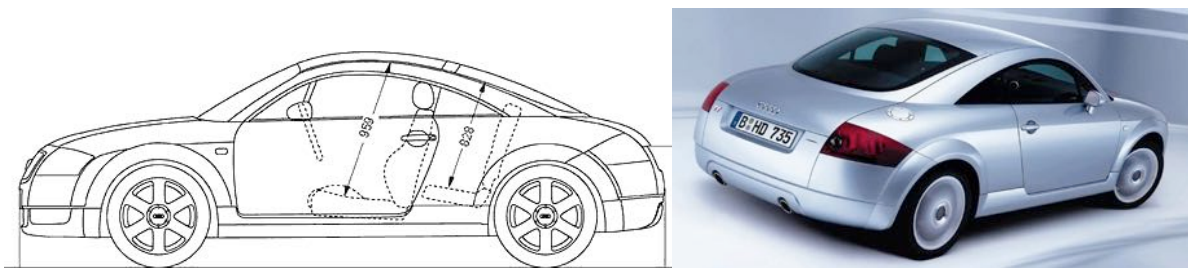
Lift

We have seen that large amounts of swept area at the rear (at low sweep angles) can introduce powerful vortices. Just like on delta wings these cause low pressure regions on the underlying surface which generate lift:



Lift as a function of rear sweep angle⁴

Also, if the swept area extends a long way (such as on a fastback design) the attached flow region in between the vortices looks not dissimilar from that seen on the rear of a highly cambered aerofoil – which would also suggest that the car produces a fair amount of lift (even without vortices). At high speeds this is bad news because it reduces friction between the tyres and the road which can lead to loss of control when cornering. A recent example is the original Audi TT:



The Audi TT (Mark I)^{}**

Aerodynamically, the rear looks very nice on this car. Surface discontinuities are avoided and the shallow angle of the rear windscreen suggests that attached flow was achieved over much of its surface (whether or not there are vortices at the sides is hard to tell). However, the large amount of attached flow – especially all the way to the boot lid, coupled with the rounded tail (which might promote even more flow attachment) caused a fair amount of lift. After a series of high-speed accidents (when drivers lost control under cornering) the car was withdrawn and re-designed. An electronic stability system was added, the suspension was modified and a rear spoiler was attached to reduce the lift:

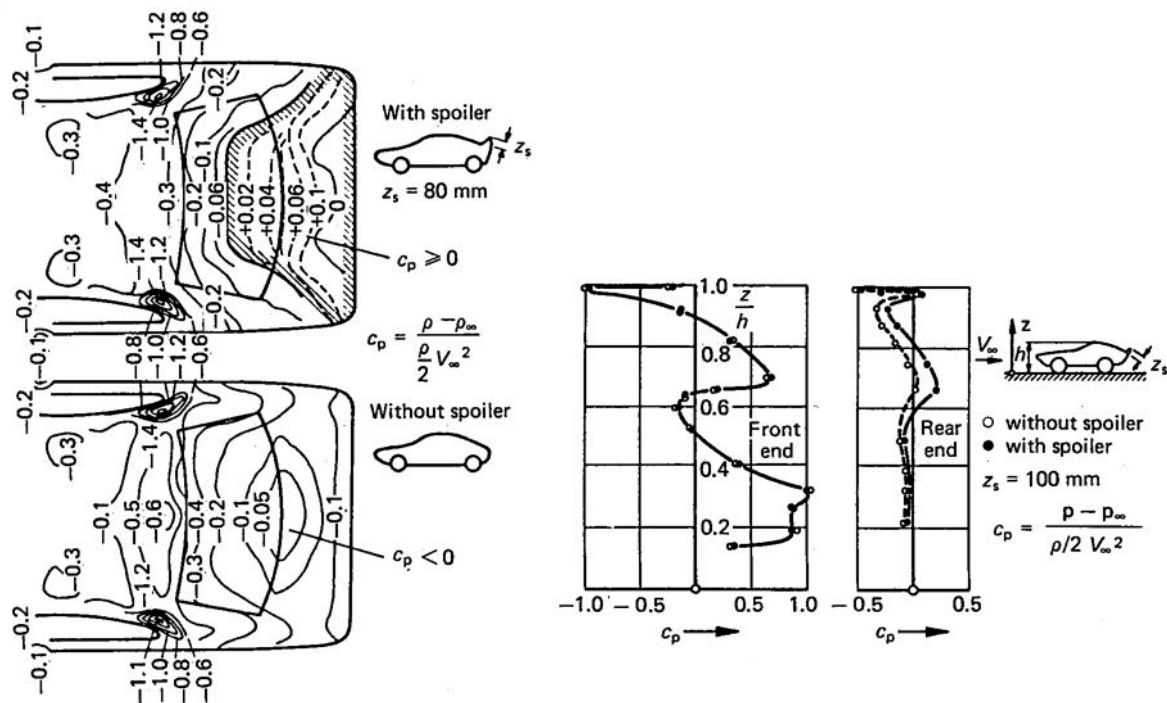
^{**} Images: <http://www.smcars.net> <http://www.imagemania.net/data/media/3/Audi%20TT%20Coupe%201%20->



The Audi TT (Mark II)**. Note the additional rear spoiler

The location of the spoiler confirms that the flow over the boot lid is attached and by fixing the separation location and re-directing the separated flow upwards a high-pressure region on the boot lid is generated which reduces the lift (in aerodynamic terms the effective camber of the car has been reduced). Note that this type of spoiler is quite different from the more subtle rear detailing discussed earlier. Here the aim is to reduce lift and improve cornering, whereas the slight concave surface discussed earlier is primarily a drag reduction device.

Pressure measurements on generic fastback shapes with and without spoiler confirm this effect:



Effect of rear spoiler on surface pressures on fastback shapes⁴

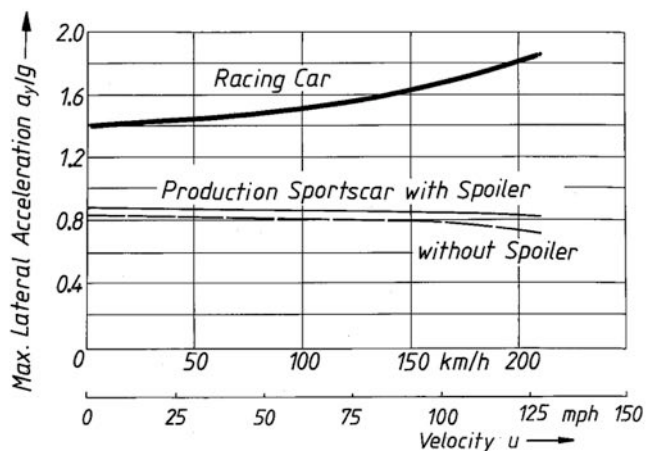
Note that the pressure is increased not only on the boot lid, but also at the rear end. This might save a bit of drag but in this case this is probably offset by the increased wake area.

Another car fitted with a spoiler to generate downforce is the Porsche 911. The original shape did not feature a spoiler whereas later versions all saw the addition of a large rear spoiler.



The Porsche 911 – note the large rear spoiler in the later version

This type of very large spoiler at the rear of a fastback design is clearly aimed at reducing lift rather than saving drag. Therefore, such spoilers are only relevant if lift is a concern – that is for fast, very streamlined, cars with large areas of attached flow all the way to the rear (and significant effective camber). Even then, the effect on cornering is quite modest for road cars:



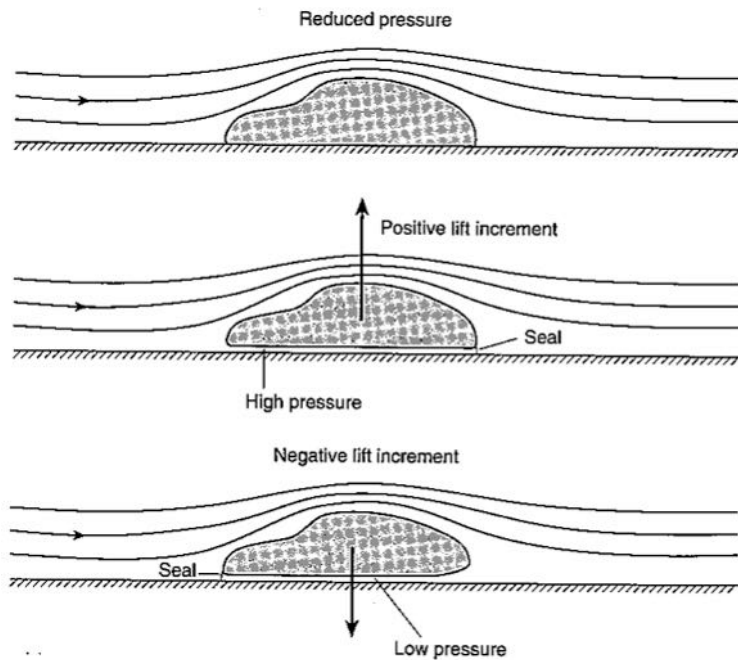
Effect of rear spoiler on cornering ability⁴

Most of the add-on spoilers you can see on ‘customised’ cars are only useful as trays for a hot drink in the car park.



Amateur aerodynamicist or boy racer?

Front spoilers can also have a significant effect on downforce by modifying the pressure below the car. This is particularly effective if combined with a rear diffuser (which further reduces underbody pressure):



Simple schematic of the effect of front and rear underbody spoiler on lift⁵

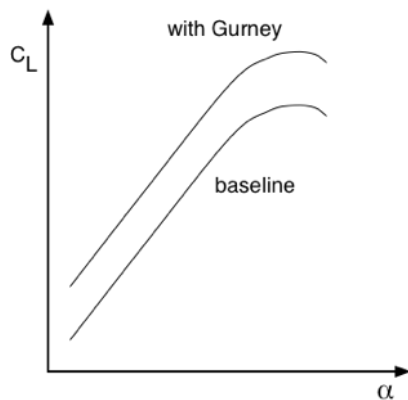
Gurney flaps

A very effective way to change the lift force of an aerofoil (or other streamlined body) was developed by the American race car team owner Dan Gurney. The device was later studied aerodynamically by Bob Liebeck who termed it ‘Gurney flap’^{††}. The device a simple right angle strip added to the trailing edge of a wing:



Simple Gurney flap to enhance lift

The effect of a Gurney flap is to increase effective camber. Because the flap also creates a thick trailing edge (which relaxes the Kutta condition) the overall aerodynamics are relatively complex and quite subtle. However, the main effect is to increase lift (albeit at the price of increased drag – but not as much as one might think).



Effect of Gurney flap on lift of an aerofoil

Gurney flaps are particularly popular on race cars because they can be applied (and removed) very quickly. During a typical Formula 1 race one can sometimes see Gurneys added or removed during a pit stop (and depending on the track they can be present at the start of the race). Below are some examples from various race-cars:



Gurney flap added to rear spoiler (see close-up on right)

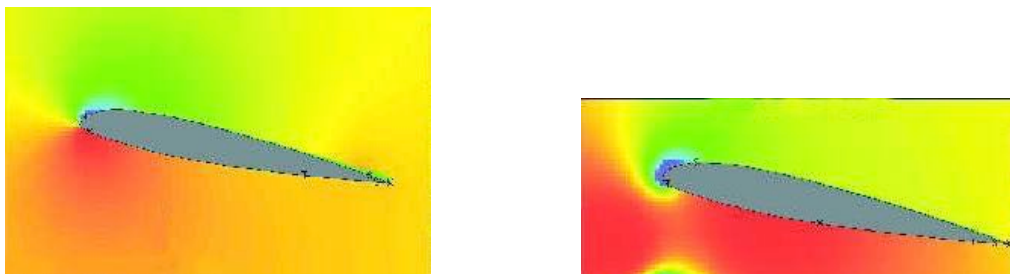
^{††} See *wikipedia* or Liebeck, R.H., “Design of Subsonic Airfoils for High Lift”, *J. Aircraft*, **15**(9), pp.547-561, Sep 1978



Large Gurney flaps on rear

Ground effect

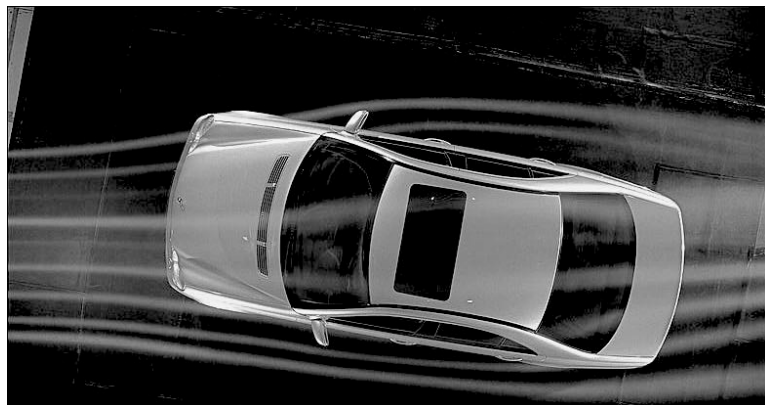
From an aerodynamicist's standpoint, cars are bluff bodies operating close to a fixed surface – thus they are under the influence of ground effect. As you have learned earlier in 3A1, the ground effect enhances any lift produced by the body shape (unfortunately this is generally not a good thing). The inviscid ground effect discussed earlier in the course (with the horseshoe vortex model) scales with the ground height divided by the wing span. Much closer to the ground there are further effects (both viscous and inviscid).



CFD simulation of a lifting aerofoil with and without the presence of a ground. Note the significantly enhanced pressure underneath the aerofoil in ground effect.

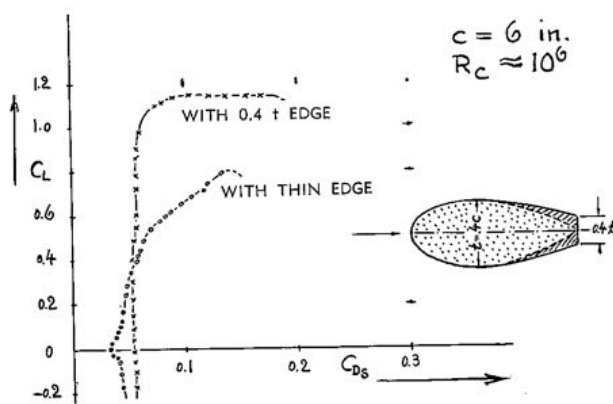
On the one hand, the mirror image under the ground plane changes the effective velocity (decreasing it in the case of a lifting body) but, more importantly, the blockage experienced underneath changes the pressure distribution which can be seen in the figure above. Here the aerofoil in ground effect shows an enhanced high pressure region below which gives significantly more lift. The vicinity to the ground generally also increases any adverse pressure gradients, causing early separation. For race cars, this can lead to a loss of downforce at low ground heights – less of a problem in road cars.

Crosswind effects



Streamlines across a car in crosswind^{††}

On windy days, the flow direction relative to the car is not always head-on. This produces an asymmetric flow over the car leading to considerable sideforce and yawing moments. Streamlined cars suffer more from this problem since they act like aerofoils. Recall that the centre of pressure on an aerofoil is around the quarter chord location – in a car this is likely to be ahead of the centre of gravity which causes a strong destabilising yawing moment. Another likely effect of cross-flow is the occurrence of flow separation which increases the drag. This can be a problem for streamlined vehicles. The image below shows how a fully streamlined shape is more sensitive to angle of attack changes than the ‘bluffer’ cut-off aerofoil:



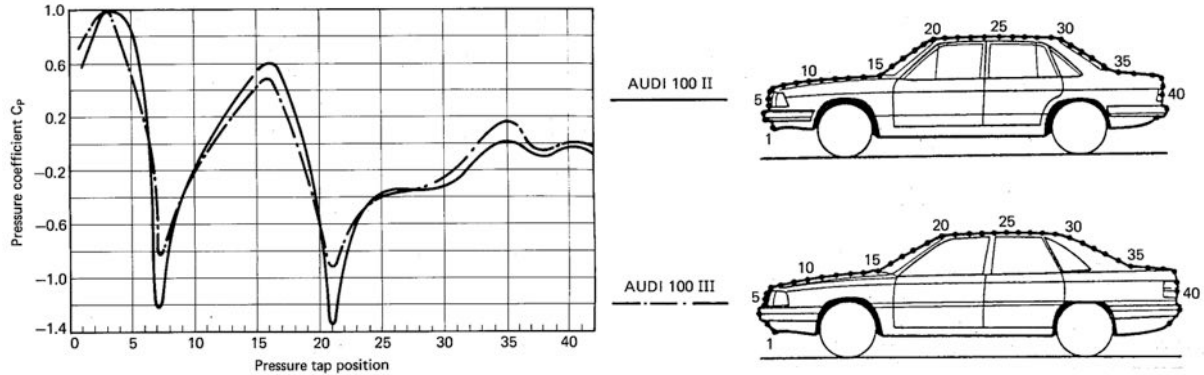
Lift and drag coefficient on aerofoils with sharp and bluff trailing edges³. The sharp trailing edge suffers from a fast increase of drag with angle of attack.

^{††} Image modified from http://us1.webpublications.com.au/static/images/articles/i1086/108676_14mg.jpg

4. Case studies

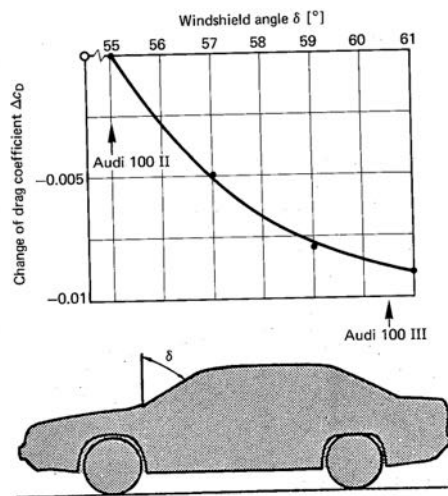
The Audi 100

The Audi 100 was considerably improved between the Mark II and Mark III models. This is apparent when comparing the pressure distribution along the centreline of the car:



Comparison of Audi 100 Mk II and Mk III centreline pressure distribution⁴

The improvements were achieved through more careful rounding of corners (larger radii), more highly swept windscreens (front and back, see also image below) and a higher boot lid. Together, these alterations reduce the low-pressure spikes which in turn limits the adverse pressure gradients immediately following the pressure minima – thus preventing separation. The base pressure (pos. 40) is also slightly improved (which helps drag).



Drag reduction due to windshield slope⁴

The Vauxhall Calibra

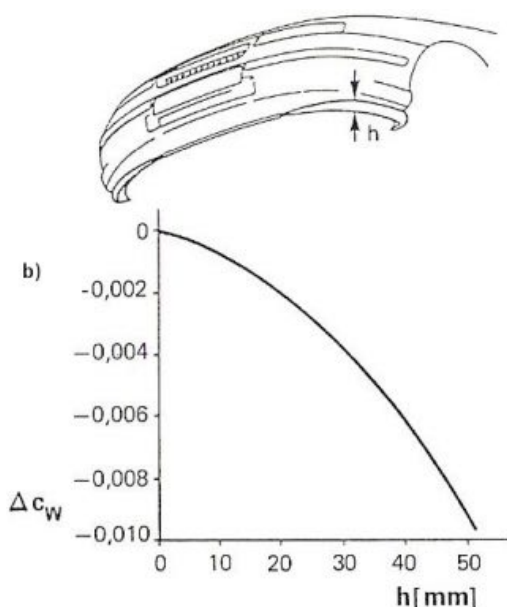
The Vauxhall Calibra achieved an impressively low drag coefficient of 0.26 in 1989 by paying careful attention to detail. If you can read German there is an excellent discussion of how this was achieved in http://www.opel-calibra.info/produktinfos_aerodynamik1.htm. Here I'll give some 'edited highlights'.



Vauxhall Calibra^{§§}

First, the basics: the car is a typical saloon shape. Noticeable is the very shallow rear window angle (the right hand photo suggests it is close to 20°). Modern production methods keep all gaps and ridges to a minimum and allow nicely rounded 'A' and 'C' pillars. Clearly the flow is expected to be attached along the rear window and onto the boot. The long slender shape (low thickness-to-chord ratio in aerofoil 'speaks') also helps. Note how the windscreens wiper is tucked behind a flow deflector.

What is particularly impressive is how small details have helped to reduce the drag.

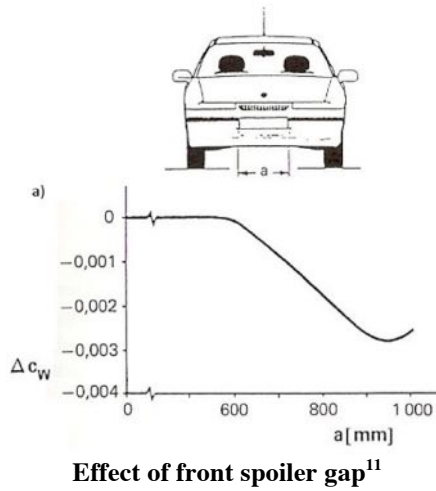


Effect of wheel deflector addition to front spoiler¹¹

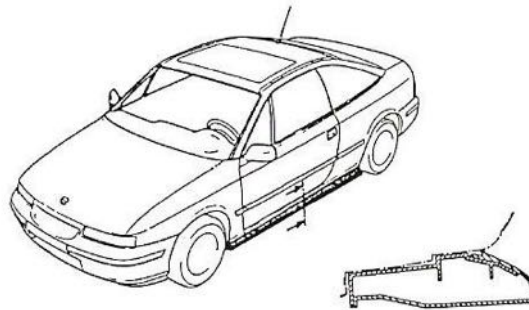
^{§§} Images: http://www.autoevolution.com/images/gallery/medium/OPELCalibra-medium-1023_4.jpg
http://www.autoevolution.com/images/gallery/medium/OPELCalibra-medium-1023_5.jpg

The front spoiler is an important part of the design. Apart from the obvious purpose to reduce the flow along the underside special side extensions shield the wheels from the oncoming flow giving additional reductions in drag as seen above (c_w is German for drag coefficient).

Somewhat counter-intuitively, a gap across the front spoiler is also reducing the drag. I can only presume that this is because the front spoiler is already optimised in the centre, and a further increase in its area is only beneficial ahead of the wheels as discussed above.

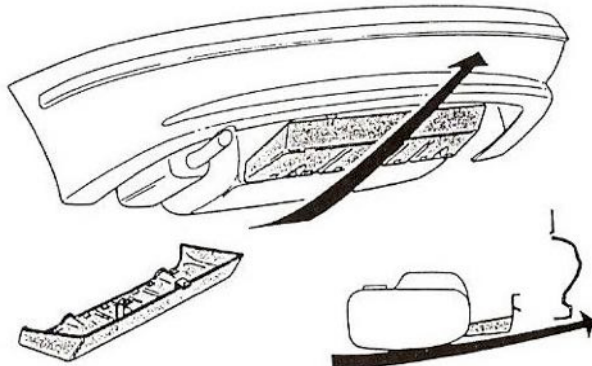


Side-skirts also reduce flow onto the underside and shield the rear wheels:



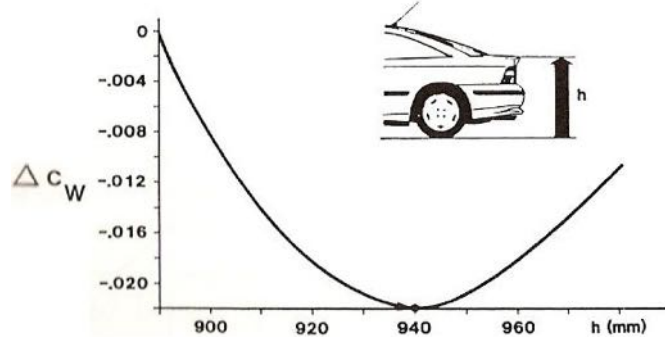
Side skirts¹¹

A rear diffuser/spoiler improves the flow across the gap between the petrol tank and the rear bumper:



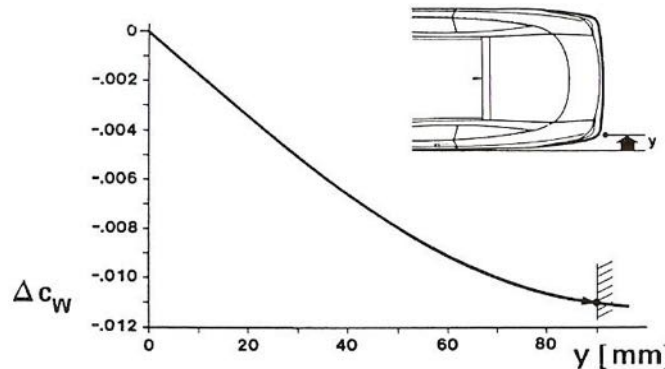
Rear underbody diffuser/spoiler¹¹

The study of tail height is interesting. When the roof height and the car length are kept constant varying the height of the boot changes the angle of the rear window. By increasing the height this angle is shallower (which is beneficial for the flow along the window) but at the same time the base area is increased (which increases drag). Therefore, there is an optimum:



Effect of boot lid height on drag¹¹

Finally, a fair amount of boat-tailing along the sides decreases the base area (and slightly increases base pressures):



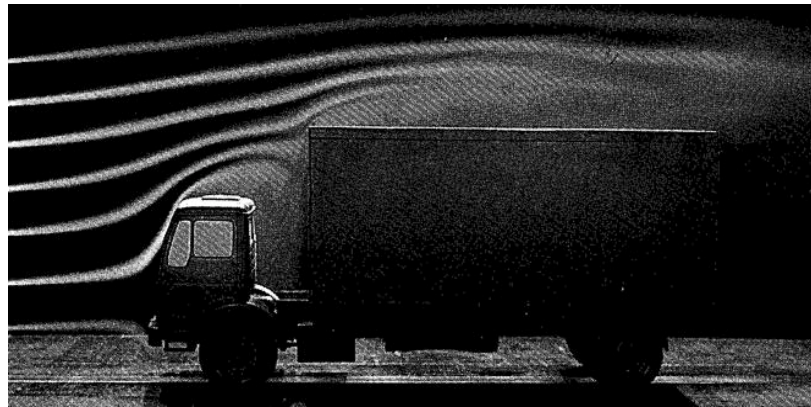
Effect of boat-tailing on the sides¹¹

Together with new production methods (at the time), which produced very smooth surfaces and good radii of curvature in the corners, the Calibra set a world record for low aerodynamic drag which remains a benchmark today (the Toyota Prius has the same drag coefficient). Wikipedia has a nice list of drag coefficients for production cars (to be taken with caution like everything on the web).

5. Commercial vehicles

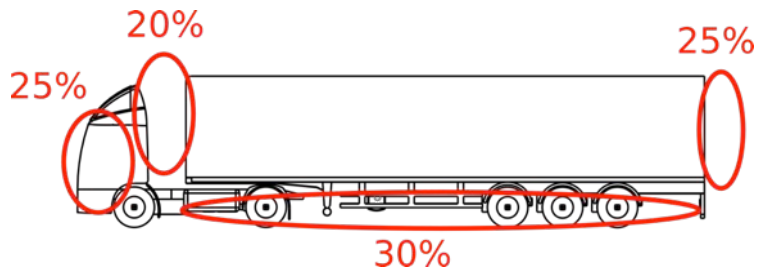
General flow features

Road haulage vehicles present obvious challenges to aerodynamicists. Here we discuss the most common variety – the ‘articulated lorry’ where a towing vehicle (‘tractor’) pulls a rectangular (semi-) ‘trailer’. Practical constraints (load volume shape and size, loading/unloading etc) make it hard/impossible to achieve an ideal aerodynamic shape:



Streamlines over a typical HGV shape⁴

The overriding flow features (and problems) are the separation behind the bluff trailer and the flow through the gap between the tractor and the trailer. Typically there are four major sources of aerodynamic drag: The towing vehicle (mainly the front and sides), the large wake, the tractor-trailer gap and the underbody. Recent literature studies by 4th year CUED students have suggested the approximate breakdown of each contribution seen below:



Approximate breakdown of aerodynamic drag contribution on a typical articulated HGV

To reduce drag we can apply some of the lessons learned from passenger vehicles. Most towing vehicles are well-designed and feature the sort of aerodynamic modifications one might expect: rounded corners (some even feature turning vanes to help the flow) and clean lines. The radiator is kept as small as possible (the large engine requires considerable cooling so this is larger than on cars). However, practical considerations limit what can be achieved. In particular, the maximum length of a truck is limited by law (the combined length of tractor and trailer) which is why designers aim to make the towing vehicle as compact as possible to maximise load space. This is different in the US where only the length of the trailer is restricted. As a result the towing vehicle is more aerodynamic with a longer ‘nose’.



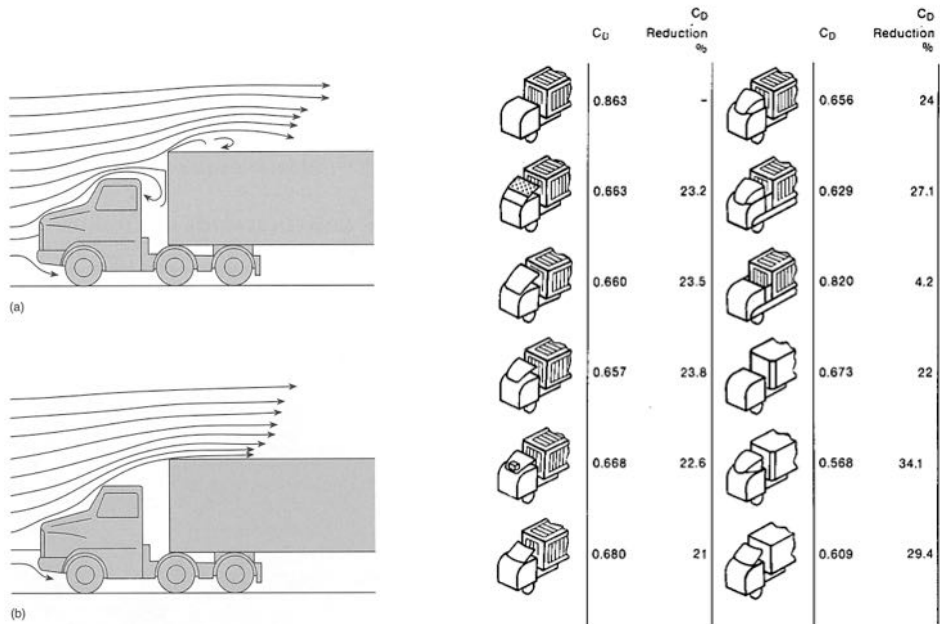
Mercedes concept tractor-trailer configuration and tractor-trailer gap treatment***

The tractor-trailer gap is a significant problem. A sizeable gap is necessary to allow tight turning circles and access for maintenance and various controls (e.g. cooling on a refrigerated trailer). The best solution are spoilers on the roof of the tractor cab which direct the flow around the trailer to reduce this problem.



Tractor-trailer gap treatment

*** Photo by Richard Stephens, CUED



Effect of cab deflectors on cab-gap flow. From 5 (left) and 4 (right)

The rear of the trailer generally features no aerodynamic treatments because it is the main access for loading/unloading. Thus streamlining, which is such a dominant feature in passenger vehicle design, is completely absent. There have been experiments with add-on devices (see below) which show considerable drag reductions but these remain impractical (and illegal because of the additional length).



Retro-fit boat-tail^{†††}

^{†††} Photo by Richard Stephens, CUED

Changing the actual shape of the trailer to incorporate a significant boat-tail generally reduces load space. Many operators use standard sized crates and even a small reduction in internal space could lead to the loss of considerable cargo by creating ‘dead space’. Aerodynamic efficiency has to be considered per cargo mass or volume and thus a more ‘aerodynamic’ shape can actually be less fuel efficient. However, a recent collaboration between the department (through 4th year projects) and Waitrose has led to the design of a trailer with very subtle boat-tailing that does not reduce internal load volume or the size of the rear cargo doors.



The CUED designed Waitrose trailer with embedded boat-tail

Modern commercial vehicles also include treatments to reduce underbody drag, similar to those found on cars. The front towing vehicle can include a small spoiler to reduce the flow towards the underside (or at least the front shape is designed to move the stagnation point down as far as possible).



Front of a modern tractor unit (left) and MAN concept vehicle (right)***

*** <http://tekniikanmaailma.fi/uutiset/manin-nakemys-tulevaisuuden-kuorma-autosta>

Another feature widely used are side-skirts on the trailer to limit the entrainment of flow from the sides into the underbody of the vehicle – these can give significant underbody drag reductions.



Side skirts on a modern trailer^{sss}

The CUED Waitrose trailers also feature extensive side-skirts (including partial skirts around the rear wheels) and all measures in combination have been found to give more than 10% reduction of aerodynamic drag and a real-world 6% fuel reduction.



Side-skirts on Waitrose trailer (folded up)

However, many commercial vehicles require considerable ground clearance which limits the extent to which front spoilers and skirts can be employed.

^{sss} Photo by Richard Stephens, CUED

Crosswind

Because heavy-goods vehicles drive relatively slowly (and largely on motorways in open countrysides) cross-winds are a considerable problem. This is exacerbated by the fact that typical lorries and trailers are tall and thus more exposed to wind than passenger cars which are closer to the ground. Below are a few figures from a report published by the UK's *Transport and Road Research Laboratory* in 1978¹² which show the prevalent wind direction across Britain and the main directions of travel for heavy goods vehicles.

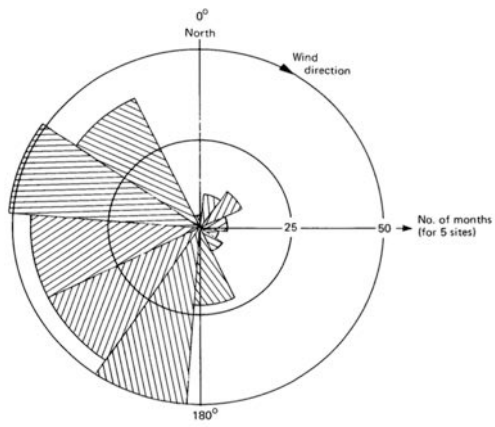


Fig. 4 WIND DIRECTION DISTRIBUTION FOR BRITAIN

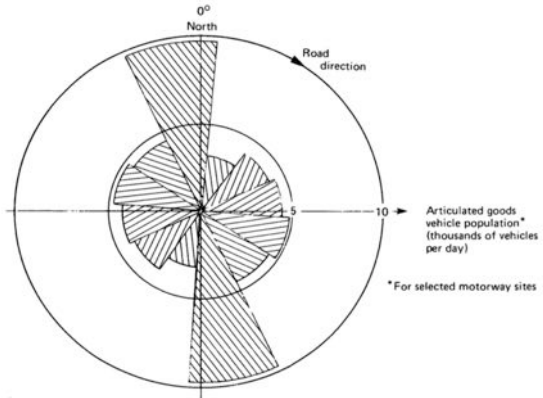
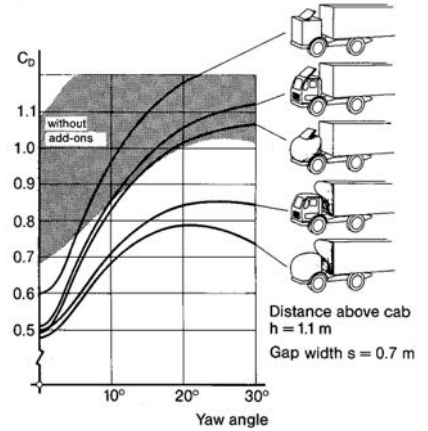
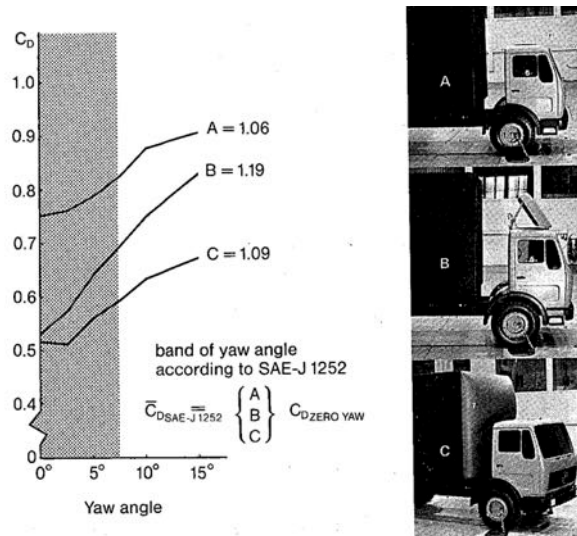
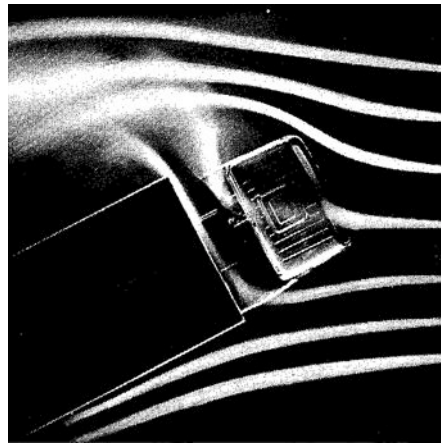


Fig. 5 ARTICULATED GOODS VEHICLE POPULATIONS FOR VARIOUS MOTORWAY DIRECTIONS

Predominant wind direction (left) and road freight driving direction (right) in the UK¹²

This shows that there is a great likelihood of cross-wind. Measurements on motorways suggest that the average wind speed is of the order of 3.5 m/s at a height of 3m above ground which is considerable compared to the average speed of trucks (around 25 m/s). Side-wind not only causes dangerous side-forces and yawing moments but there is also a significant detrimental effect on drag. This is because the bluff shape of a typical trailer experiences considerable additional separation when yawed. Also, cross-winds induce flow through the tractor-trailer gap which further increases drag. Therefore, drag measurements on heavy goods vehicles normally include various yaw angles to produce a '*wind-averaged*' *drag coefficient*. Here, drag measurements are taken at a variety of yaw angles and a weighted average is calculated which is representative of a real world operation in the UK. However, this is an expensive and time-consuming procedure and in practice it has been shown that a single measurement at a yaw angle of 5° is reasonably representative of most circumstances.

Because of the significance of cross-wind it is important for drag reduction devices such as spoilers to be robust to yaw which explains the recent trend towards more 3-dimensional designs. As seen below, a spoiler performing poorly in cross-wind can actually make drag worse.



Various spoiler designs and their sensitivity to cross-wind⁴

References:

- ¹ Fluid Mechanics, Frank M. White, 4th ed. (McGraw-Hill series in mechanical engineering), 1999
- ² Aerodynamics for Engineering Students, E.L. Houghton and P.W. Carpenter, 4th Rev. ed. (Edward Arnold), 1993
- ³ Fluid-Dynamic Drag, S.F. Hoerner, Published by the Author (Hoerner Fluid Dynamics), 1992
- ⁴ Aerodynamics of Road Vehicles: from fluid mechanics to vehicle engineering, ed. W.-H. Hucho, 4th ed., Society of Automotive Engineers, Inc. 1998
- ⁵ Road Vehicle Aerodynamic Design, R.H. Barnard, (MechAero Publishing, St Albans) 2009
- ⁶ Luftwiderstand von Personenwagen, W.-H. Hucho, AdK, Essen 1978, Chapter 4
- ⁷ Aerodynamics - The Science of air in Motion, John E. Allen, p.90, Allen Brothers and Father, Blythborough, Suffolk, 2nd ed. 1982
- ⁸ P.W. Bearman, Bluff body flows applicable to vehicle aerodynamics. ASME J. Fluids Engineering, Vol. 102, pp. 265-274, 1980.
- ⁹ P.W. Bearman, Bluff body flows applicable to vehicle aerodynamics. ASME J. Fluids Engineering, Vol. 102, pp. 265-274, 1980.
- ¹⁰ Conan et al, Experimental aerodynamic study of a car-type bluff body, Exp Fluids 50:1273-1284, 2011
- ¹¹ http://www.opel-calibra.info/produktinfos_aerodynamik1.htm
- ¹² Ingram, K.C., "The wind-averaged drag coefficient applied to heavy goods vehicles", Supplementary report 392, Transport and Road Research Laboratory, Crowthorne, Berkshire, 1978